Electronic Supplementary Material (ESI) for Dalton Transactions.
This journal is © The Royal Society of Chemistry 2017

Electronic Supplementary Information (ESI) for:

Mono- and bimetallic manganese–carbonyl complexes and clusters bearing imidazol(in)ium-2-dithiocarboxylate ligands

Tomás F. Beltrán,[a] Guillermo Zaragoza,[b] and Lionel Delaude[*a]

[a]*Laboratory of Organometallic Chemistry and Homogeneous Catalysis, Institut de chimie (B6a), Allée du six Août 13, Quartier Agora, Université de Liège, 4000 Liège, Belgium*

[b]*Unidade de Difracción de Raios X, Edificio CACTUS, Universidade de Santiago de Compostela, Campus Vida, 15782 Santiago de Compostela, Spain*

Table of content

Part 1 - Experimental Procedures

1. General Information

All the reactions were carried out using standard Schlenk techniques under a dry argon atmosphere. Solvents were distilled from appropriate drying agents and deoxygenated prior to use. Manganese(I) pentacarbonyl bromide, decacarbonyldimanganese(0), and sodium-mercury amalgam (4–5% Na) were purchased from Strem. The NHC·CS_2 zwitterions were prepared according to literature.[1] Unless otherwise specified, ^{1}H and ^{13}C{^{1}H} NMR spectra were recorded at 298 K with Bruker Avance 250 or DRX 400 spectrometers. Chemical shifts are listed in parts per million downfield from TMS and are referenced from the solvent peaks or TMS. Infrared spectra were recorded with a Bruker Equinox 55 FT–IR spectrometer. UV/visible spectra were recorded with a Hewlett–Packard HP 8453 spectrophotometer. Electrospray mass spectra were obtained using a Micromass LCT Premier instrument. Elemental analyses were carried out in the Laboratory of Pharmaceutical Chemistry at the University of Liège.

2. Synthesis of Mononuclear [MnBr(CO)$_3$(S$_2$C·NHC)] Complexes 1–5

A 50 mL two-neck round-bottomed flask equipped with a magnetic stirring bar and a three-way stopcock was loaded with [MnBr(CO)$_5$] (27.49 mg, 0.100 mmol) and a NHC·CS_2 zwitterion (0.105 mmol). The reactor was purged of air by applying three vacuum/argon cycles before dry CS_2 (15 mL) was added. The reaction mixture was heated in an oil bath at 60 ºC for 1 h leading to a dark colored suspension, which was cooled to room temperature and filtered with suction. The precipitate was washed with *n*-pentane (20 mL) and dried under high vacuum to afford complexes **1–5**.

[MnBr(CO)$_3$(S$_2$C·ICy)] (1). Purple microcrystalline solid (0.0284 g, 54% yield). ^{1}H NMR (250 MHz, CD_2Cl_2): δ 0.87–2.18 (m, 20 H, Cy), 4.79 (br m, 2 H, CHN), 7.21 ppm (s, 2 H, =CHN). ^{13}C NMR (100 MHz, CD_2Cl_2): δ 25.3 (CH_2), 25.4 (CH_2), 34.5 (CH_2), 59.1 (=CHN), 118.9 (Im-C^{4,5}), 142.1 (Im-C^2), 221.6 ppm (CS_2). IR (KBr): ν_{CO} 2016 (s), 1925 (s), 1909 (s) cm^{-1}. UV/Vis (EtOH): λ_{max} (ε) 271 (7400), 351 nm (4300 M^{-1} cm^{-1}). ESI-MS (CH_3CN) *m/z*: calcd for $C_{19}H_{24}N_2O_3MnS_2$ ([M–Br]$^+$), 447.0603; found, 447.0606. Anal. calcd for $C_{19}H_{24}BrN_2O_3MnS_2$ (527.38): C, 43.27; H, 4.59; N, 5.31; S, 12.16; found C, 43.31; H, 4.94; N, 5.78; S, 11.94.

[MnBr(CO)$_3$(S$_2$C·IMes)] (2). Blue-green microcrystalline solid (0.0486 g, 81% yield). ^{1}H NMR (250 MHz, CD_2Cl_2): δ 2.18 (br s, 12 H, *ortho*-CH_3), 2.40 (br s, 6 H, *para*-CH_3), 7.09 (br s, 4 H, *meta*-CH), 7.29 ppm (br s, 2 H, =CHN). ^{13}C NMR (100 MHz, CD_2Cl_2): δ 18.4 (CH_3), 21.6 (CH_3),

124.2 (Im-$C^{4,5}$) 130.3 (C_{ar}), 131.3 (C_{ar}), 135.4 (C_{ar}), 138.0 (C_{ar}), 142.3 (Im-C^2), 215.5 ppm (CS_2). IR (KBr): ν_{CO} 2013 (s), 1936 (s), 1900 (s) cm^{-1}. UV/Vis (EtOH): λ_{max} (ε) 272 (8300), 364 (4100), 605 nm (1200 M^{-1} cm^{-1}). ESI-MS (CH_3CN) *m/z*: calcd for $C_{25}H_{24}MnN_2O_3S_2$ ([M–Br]$^+$) 519.0603; found, 519.0604. Anal. calcd for $C_{25}H_{24}BrMnN_2O_3S_2$ (599.44): C, 50.09; H, 4.04; N, 4.67; S, 10.70; found C, 50.46; H, 3.87; N, 4.63; S 11.14.

[MnBr(CO)$_3$(S$_2$C·IDip)] (3). Blue-green microcrystalline solid (0.0507 g, 74% yield). ^{1}H NMR (250 MHz, CD_2Cl_2): δ 1.21 (br d, $^3J_{H,H}$ = 5.0 Hz, 12 H, CH(C*H*$_3$)$_2$), 1.38 (br d, $^3J_{H,H}$ = 7.5 Hz, 12 H, CH(C*H*$_3$)$_2$), 2.51 (br m, 4 H, C*H*(CH$_3$)$_2$), 7.37 (br s, 4 H, *meta*-CH), 7.40 (br s, 2 H, =CHN), 7.62 ppm (t, $^3J_{H,H}$ = 7.5 Hz, 2 H, *para*-CH). ^{13}C NMR (100 MHz, CD_2Cl_2): δ 23.0 (CH$_3$), 25.7 (CH$_3$), 30.2 ((CH$_3$)$_2$*C*H), 124.8 (Im-$C^{4,5}$), 125.5 (C_{ar}), 131.2 (C_{ar}), 132.7 (C_{ar}), 138.6 (C_{ar}), 145.9 (Im-C^2), 214.5 ppm (CS_2). IR (KBr): ν_{CO} 2014 (s), 1937 (s), 1898 (s) cm^{-1}. UV/Vis (EtOH): λ_{max} (ε) 272 (7200), 359 (3300), 626 nm (1000 M^{-1} cm^{-1}). ESI-MS (CH_3CN) *m/z*: calcd for $C_{31}H_{36}MnN_2O_3S_2$ ([M–Br]$^+$) *m/z* = 603.1542, found 603.1542. Elemental analysis calcd for $C_{31}H_{36}BrMnN_2O_3S_2$ (683.60): C 54.47, H 5.31, N 4.10, S 9.11; found C 53.77, H 5.31, N 4.59, S 9.23.

[MnBr(CO)$_3$(S$_2$C·SIMes)] (4). Blue-green microcrystalline solid (0.0571 g, 95% yield). ^{1}H NMR (250 MHz, CD_2Cl_2): δ 2.33 (br s, 6 H, *para*-CH$_3$), 2.41 (br s, 12 H, *ortho*-CH$_3$), 4.31 (br s, 4 H, CH$_2$), 7.00 ppm (br s, 4 H, *meta*-CH). ^{13}C NMR (100 MHz, CD_2Cl_2): δ 19.0 (CH$_3$), 21.4 (CH$_3$), 51.0 (CH$_2$N), 130.5 (C_{ar}), 131.1 (C_{ar}), 136.1 (C_{ar}), 141.3 (C_{ar}), 155.5 (Im-C^2), 216.4 ppm (CS_2). IR (KBr): ν_{CO} 2014 (s), 1938 (s), 1906 (s) cm^{-1}. UV/Vis (EtOH): λ_{max} (ε) 272 (10200), 359 (6400), 586 nm (600 M^{-1} cm^{-1}). ESI-MS (CH_3CN) *m/z*: calcd for $C_{25}H_{26}MnN_2O_3S_2$ ([M–Br]$^+$) *m/z* = 521.0760, found 521.0755. Elemental analysis calcd for $C_{25}H_{26}BrMnN_2O_3S_2$ (601.46): C, 49.92; H, 4.36; N, 4.66; S, 10.66; found C, 49.42; H, 4.37; N, 4.93; S, 10.72.

[MnBr(CO)$_3$(S$_2$C·SIDip)] (5). Blue-green microcrystalline solid (0.058 g, 85% yield). ^{1}H NMR (250 MHz, CD_2Cl_2): δ 1.33 (br s, 12 H, CH(C*H*$_3$)$_2$), 1.43 (br s, 12 H, CH(C*H*$_3$)$_2$), 3.10 (br s, 4 H, C*H*(CH$_3$)$_2$), 4.35 (br s, 4 H, CH$_2$), 7.30 (br d, $^3J_{H,H}$ = 7.5 Hz, 4 H, *meta*-CH), 7.50 ppm (br t, $^3J_{H,H}$ = 7.5 Hz, 2 H, *para*-CH). ^{13}C NMR (100 MHz, CD_2Cl_2): δ 23.4 (CH$_3$), 26.6 (CH$_3$), 29.5 ((CH$_3$)$_2$*C*H), 51.8 (CH$_2$N), 125.4 (C_{ar}), 130.4 (C_{ar}), 131.4 (C_{ar}), 146.5 (C_{ar}), 176.8 (Im-C^2), 215.0 ppm (CS_2). IR (KBr): ν_{CO} 2014 (s), 1943 (s), 1899 (s) cm^{-1}. UV/Vis (EtOH): λ_{max} (ε) 273 (8800), 361 nm (5000 M^{-1} cm^{-1}). ESI-MS (CH_3CN) *m/z*: calcd for $C_{31}H_{38}MnN_2O_3S_2$ ([M–Br]$^+$) *m/z* = 605.1699, found 605.1716. Elemental analysis calcd for $C_{31}H_{38}BrMnN_2O_3S_2$ (685.62): C, 54.31; H, 5.59; N, 4.09; S, 9.35; found C, 53.79; H, 5.51; N, 4.37; S, 9.63.

3. Synthesis of Binuclear $[Mn_2(CO)_6(S_2C{\cdot}NHC)]$ Complexes 6–10 via ligand substitution

A 50 mL two-neck round-bottomed flask equipped with a magnetic stirring bar and a three-way stopcock was loaded with $[Mn_2(CO)_{10}]$ (38.99 mg, 0.100 mmol) and a NHC·CS_2 zwitterion (0.100 mmol). The reactor was purged of air by applying three vacuum/argon cycles before dry toluene (20 mL) was added. The magnetically stirred suspension was heated in an oil bath at 125 °C for 1 h (for complexes **6–8**) or 4 h (for complexes **9** and **10**). The mixture was cooled to room temperature. After evaporation of the solvent in vacuo, the residue was taken up with dichloromethane (3 mL) and filtered through a short plug of Celite, which was subsequently rinsed with dichloromethane (2 × 1 mL). The filtrate was slowly poured into *n*-heptane (80 mL) under vigorous stirring. Partial evaporation of the solvent in vacuo (to *ca*. one third of the initial volume) yielded a suspension, which was filtered with suction. The solid was washed with *n*-heptane (20 mL) and dried under high vacuum to afford complexes **6–10**.

$[Mn_2(CO)_6(S_2C{\cdot}ICy)]$ (6). Orange microcrystalline solid (0.0499 g, 85% yield). ^{1}H NMR (400 MHz, CD_2Cl_2): δ 1.21–1.31 (m, 2 H, Cy), 1.57–1.71 (m, 8 H, Cy), 1.81–1.84 (br d, 2 H, Cy), 1.94–1.97 (br d, 4 H, Cy), 2.11–2.14 (br d, 4 H, Cy), 5.42 (m, 2 H, CHN Cy), 7.18 ppm (s, 2 H, =CHN). ^{13}C NMR (100 MHz CD_2Cl_2,): δ 25.4 (CH_2), 25.7 (CH_2), 34.4 (CH_2), 58.2 (CHN), 89.3 (CS_2), 118.5 (Im-$C^{4,5}$), 146.2 (Im-C^2), 225.3 ppm (CO). IR (KBr): ν_{CO} 2013 (s), 1981 (s), 1921 (s), 1899 (s), 1884 (s) cm^{-1}. UV/Vis (EtOH): λ_{max} (ε) 273 (8800), 334 (7200), 489 nm (1400 M^{-1} cm^{-1}). ESI-MS ($C_2H_4Cl_2$) *m/z*: calcd for $C_{22}H_{24}O_6Mn_2N_2S_2$ ([M]$^+$), 585.9831; found, 585.9844. Anal. calcd for $C_{22}H_{24}N_2O_6Mn_2S_2$ (586.65): C, 45.06; H, 4.13; N, 4.78; S, 10.93. Found: C, 45.06; H, 4.18; N, 4.91; S, 10.86.

$[Mn_2(CO)_6(S_2C{\cdot}IMes)]$ (7). Red microcrystalline solid (0.0293 g, 45 % yield). ^{1}H NMR (400 MHz, CD_2Cl_2): δ 2.20 (s, 12 H, *ortho*-CH_3), 2.36 (s, 6 H, *para*-CH_3), 6.99 (s, 2 H, =CHN), 7.06 ppm (s, 4 H, *meta*-CH). ^{13}C NMR (100 MHz, CD_2Cl_2): δ 18.5 (CH_3), 21.5 (CH_3), 87.6 (CS_2), 122.7 (C_{ar}) 130.5 (C_{ar}), 131.7 (C_{ar}), 135.6 (C_{ar}), 142.0 (C_{ar}), 151.1 (Im-C^2), 227.4 ppm (CO). IR (KBr): ν_{CO} 2018 (s), 1973 (s), 1914 (s), 1884 (s) cm^{-1}. UV/Vis (EtOH): λ_{max} (ε) 273 (10200), 352 (12000), 509 nm (2000 M^{-1} cm^{-1}). ESI-MS ($C_2H_4Cl_2$) *m/z*: calcd for $C_{28}H_{24}N_2O_6Mn_2S_2$ ([M]$^+$), 657.9831, found 657.9826. Anal. calcd for $C_{28}H_{24}N_2O_6Mn_2S_2$ (658.51): C, 51.07; H, 3.67; N, 4.25; S 9.74; found C, 50.83; H, 3.86; N, 4.58; S, 9.52.

$[Mn_2(CO)_6(S_2C{\cdot}IDip)]$ (8). Red microcrystalline solid (0.0540 g, 73 % yield). ^{1}H NMR (400 MHz, CD_2Cl_2): δ 1.17 (d, $^3J_{H,H}$ = 6.4 Hz, 12 H, CH(CH_3)$_2$), 1.51 (d, $^3J_{H,H}$ = 6.3 Hz, 12 H, CH(CH_3)$_2$), 2.57 (m, 4 H, C*H*(CH_3)$_2$), 7.07 (s, 2 H, =CHN), 7.36 (d, $^3J_{H,H}$ = 7.6 Hz, 4 H, *meta*-CH),

7.57 ppm (t, $^3J_{H,H}$ = 7.6 Hz, 2 H, *para*-CH). ^{13}C NMR (100 MHz, CD_2Cl_2): δ 22.8 (CH_3), 25.8 (CH_3), 30.1 ($(CH_3)_2CH$), 87.3 (CS_2) 124.1 (C_{ar}), 125.3 (C_{ar}), 131.9 (C_{ar}), 132.4 (C_{ar}), 146.3 (C_{ar}), 152.8 (Im-C^2), 224.7 ppm (br, CO). IR (KBr): ν_{CO} 2015 (s), 1977 (s), 1934 (s), 1907 (s), 1883 (s) cm^{-1}. UV/Vis (EtOH): λ_{max} (ε) 272 (8300), 350 (10200), 511 nm (1600 M^{-1} cm^{-1}). ESI-MS ($C_2H_4Cl_2$) *m/z*: calcd for $C_{34}H_{36}N_2O_6Mn_2S_2$ ($[M]^+$), 742.0770; found, 742.0760. Anal. calcd for $C_{34}H_{36}N_2O_6Mn_2S_2$ (742.68): C, 54.98; H, 4.89; N, 3.77; S, 8.63. Found: C, 54.69; H, 4.91; N, 3.84; S, 8.20.

$Mn_2(CO)_6(S_2C{\cdot}SIMes)]$ (9). Red microcrystalline solid (0.0418 g, 63 % yield). ^{1}H NMR (400 MHz, CD_2Cl_2): δ 2.31 (s, 6 H, *para*-CH_3), 2.40 (s, 12 H, *ortho*-CH_3), 3.97 (s, 4 H, CH_2), 6.99 ppm (s, 4 H, *meta*-CH). ^{13}C NMR (100 MHz, CD_2Cl_2): δ 18.7 (CH_3), 21.4 (CH_3), 50.9 (CH_2N), 85.9 (CS_2), 130.7 (C_{ar}), 132.9 (C_{ar}), 136.0 (C_{ar}), 140.7 (C_{ar}), 168.9 (Im-C^2), 223.4 ppm (CO). IR (KBr): ν_{CO} 2019 (s), 1978 (s), 1930 (s), 1908 (s), 1884 (s) cm^{-1}. UV/Vis (EtOH): λ_{max} (ε) 275 (10900), 346 (10800), 518 nm (1600 M^{-1} cm^{-1}). ESI-MS ($C_2H_4Cl_2$) *m/z*: calcd for $C_{28}H_{26}N_2O_6Mn_2S_2$ ($[M]^+$), 659.9988; found, 659.9995. Anal. Calcd for $C_{28}H_{26}N_2O_6Mn_2S_2$ (660.52): C, 50.91; H, 3.97; N, 4.24; S, 9.71; found C, 50.13; H, 4.36; N, 4.81; S, 9.14.

$[Mn_2(CO)_6(S_2C{\cdot}SIDip)]$(10). Red microcrystalline solid (0.0296 g, 40% yield). ^{1}H NMR (400 MHz, CD_2Cl_2): δ 1.30 (d, $^3J_{H,H}$ = 6.8 Hz, 12 H, $CH(CH_3)_2$), 1.56 (d, $^3J_{H,H}$ = 6.7 Hz, 12 H, $CH(CH_3)_2$), 3.05 (sept, $^3J_{H,H}$ = 6.8 Hz, $^3J_{H,H}$ = 6.7 Hz, 4 H, $CH(CH_3)_2$), 4.08 (s, 4 H, CH_2), 7.29 (d, $^3J_{H,H}$ = 7.8 Hz, 4 H, *meta*-CH), 7.45 ppm (t, $^3J_{H,H}$ = 7.8 Hz, 2 H, *para*-CH). ^{13}C NMR (100 MHz, CD_2Cl_2): δ 23.5 (CH_3), 26.7 (CH_3), 30.0 ($(CH_3)_2CH$), 58.2 (CH_2N), 85.4 (CS_2), 125.6 (C_{ar}), 131.3 (C_{ar}), 133.4 (C_{ar}), 147.0 (C_{ar}), 169.8 (Im-C^2), 220.5 ppm (CO). IR (KBr): ν_{CO} 2019 (s), 1980 (s), 1936 (s), 1919 (s), 1888 (s) cm^{-1}. UV/Vis (EtOH): λ_{max} (ε) 277 (12800), 345 (9500), 510 nm (1400 M^{-1} cm^{-1}). ESI-MS ($C_2H_4Cl_2$) *m/z*: calcd for $C_{34}H_{38}N_2O_6Mn_2S_2$ ($[M]^+$), 744.0927; found 744.0855. Anal. calcd for $C_{34}H_{38}N_2O_6Mn_2S_2$ (744.68): C, 54.84; H, 5.14; N, 3.76; S, 8.61. Found: C, 54.66; H, 5.57; N, 4.03; S, 8.14.

4. Synthesis of Binuclear $[Mn_2(CO)_6(S_2C{\cdot}NHC)]$ Complexes 7 and 8 via comproportionation–decarbonylation

A solution of $Na[Mn(CO)_5]$ was prepared by stirring a mixture of $[Mn_2(CO)_{10}]$ (23.4 mg, 0.060 mmol) and an excess of Na–Hg amalgam (4–5 weight-% of Na, 0.1540 g, *ca.* 6 equiv.) in dry THF (15 mL) for 40 min at room temperature. The yellow supernatant solution was transferred with a cannula into a slurry of $[MnBr(CO)_3(S_2C{\cdot}IMes)]$ (**2**, 59.9 mg, 0.1 mmol) or $[MnBr(CO)_3$-$(S_2C{\cdot}IDip)]$ (**3**, 68.4 mg, 0.1 mmol) in dry THF (5 mL). The reaction mixture was heated in an oil

bath at 70 ºC for 1 h. After evaporation of the solvent in vacuo, the residue was taken up with dichloromethane (3 mL) and filtered through a short plug of Celite. The inorganic salts were rinsed with dichloromethane (2 × 1 mL) and the filtrate was slowly poured into *n*-heptane (80 mL) under vigorous stirring. Partial evaporation of the solvent in vacuo (to *ca*. one half of the initial volume) yielded a suspension, which was filtered with suction. The precipitate was washed with *n*-heptane (20 mL) and dried under high vacuum to afford complexes **7** and **8** in 49% and 47% yields, respectively. Analytical data were identical to those listed in the previous section.

Part 2 – NMR Spectra

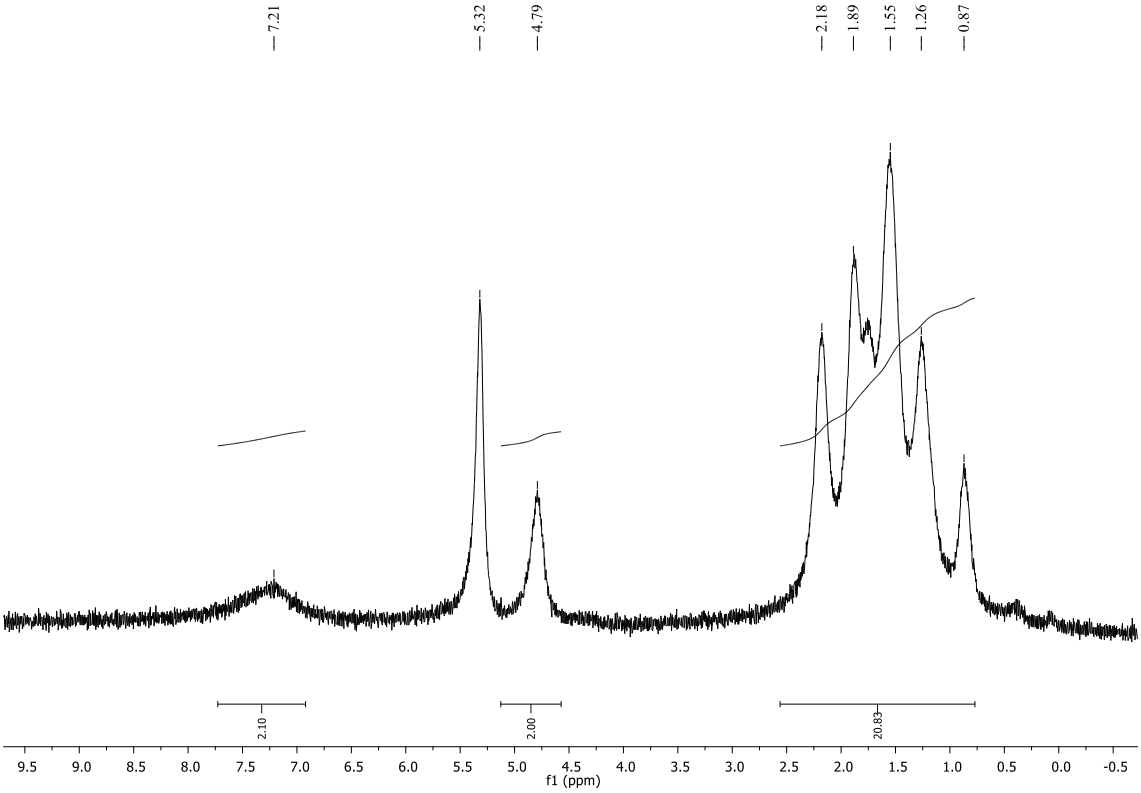

Figure S1. ^{1}H NMR spectrum (250 MHz, CD_2Cl_2, 298 K) of $[MnBr(CO)_3(S_2C{\cdot}ICy)]$ (**1**)

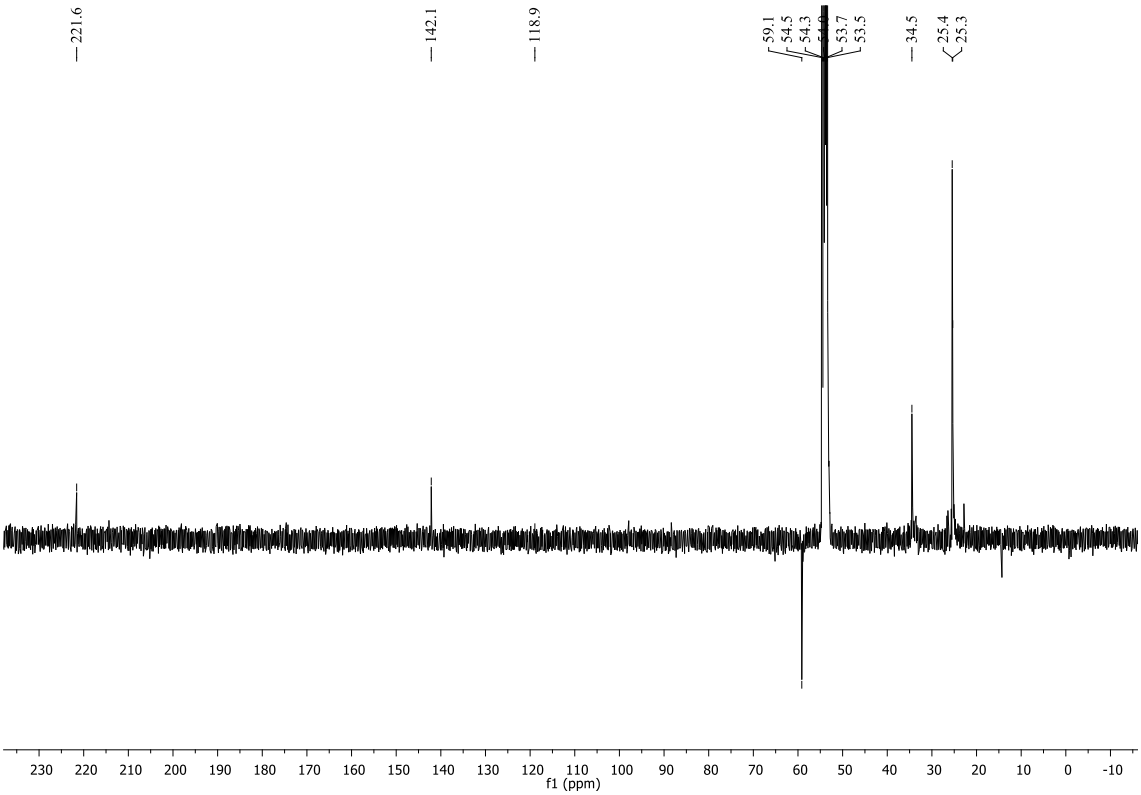

Figure S2. ^{13}C NMR spectrum (100 MHz, CD_2Cl_2, 273 K) of $[MnBr(CO)_3(S_2C{\cdot}ICy)]$ (**1**)

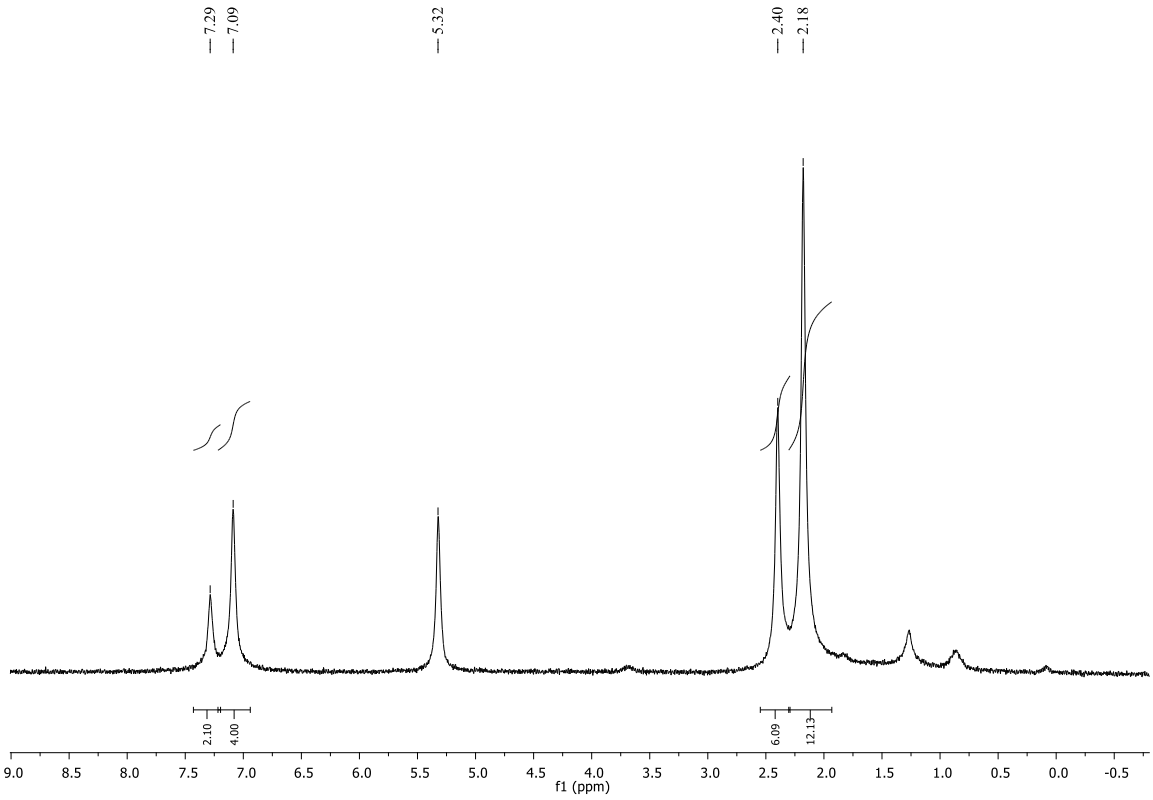

Figure S3. ^{1}H NMR spectrum (250 MHz, CD_2Cl_2, 298 K) of [$MnBr(CO)_3(S_2C{\cdot}IMes)$] (**2**)

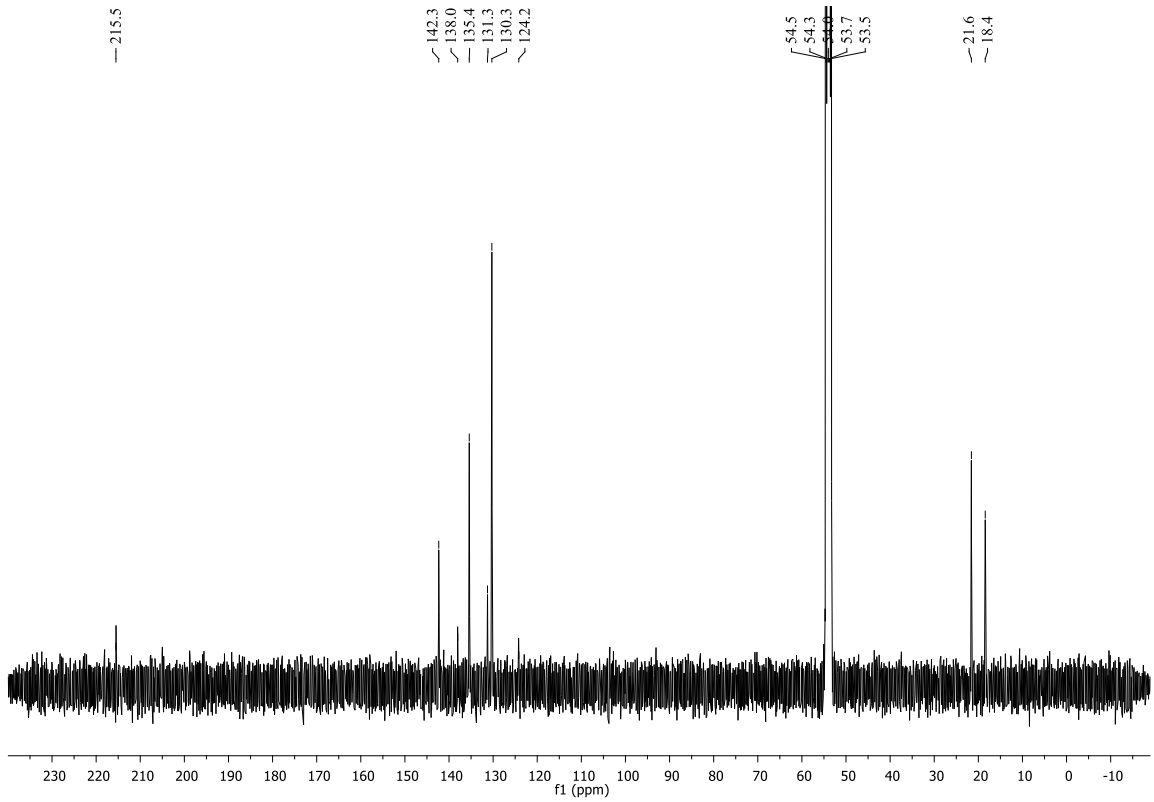

Figure S4. ^{13}C APT NMR spectrum (100 MHz, CD_2Cl_2, 298 K) of [$MnBr(CO)_3(S_2C{\cdot}IMes)$] (**2**)

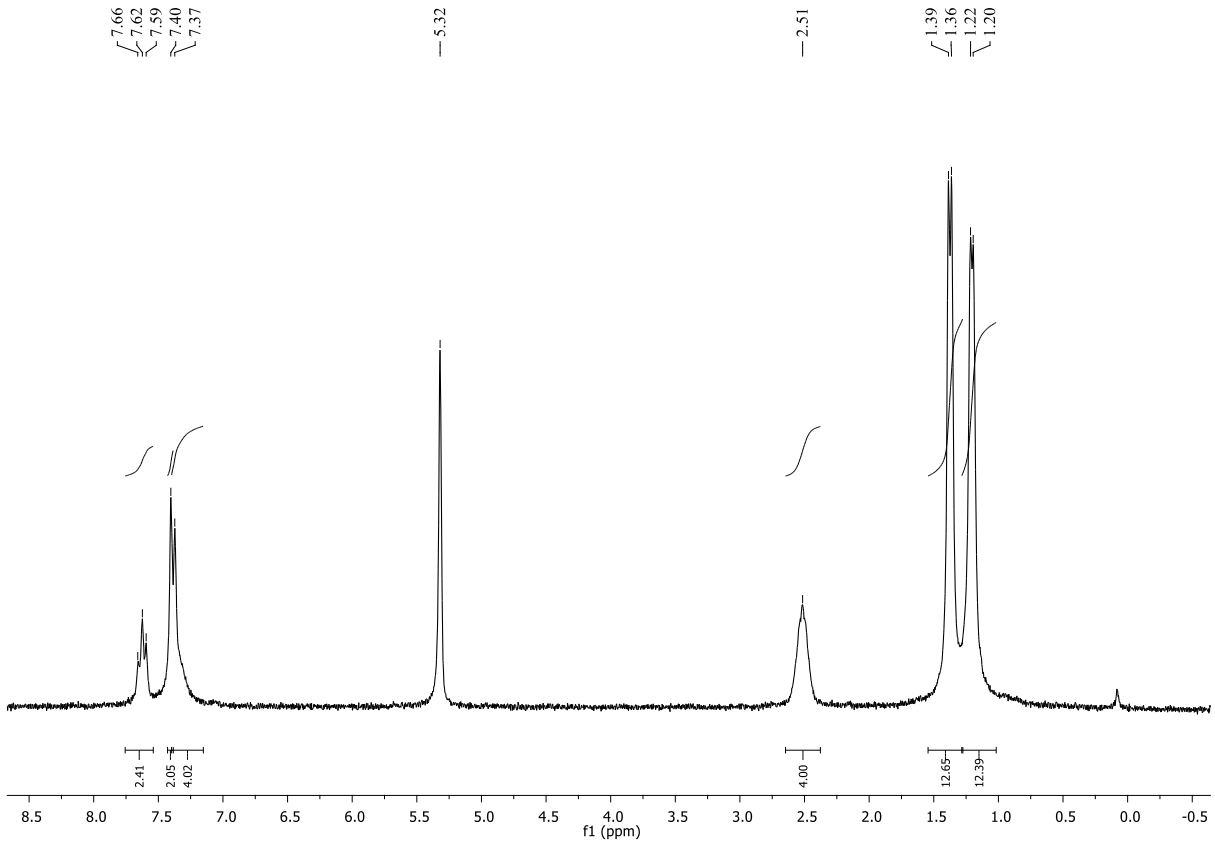

Figure S5. ^{1}H NMR spectrum (250 MHz, CD_2Cl_2, 298 K) of [MnBr(CO)$_3$(S$_2$C·IDip)] (**3**)

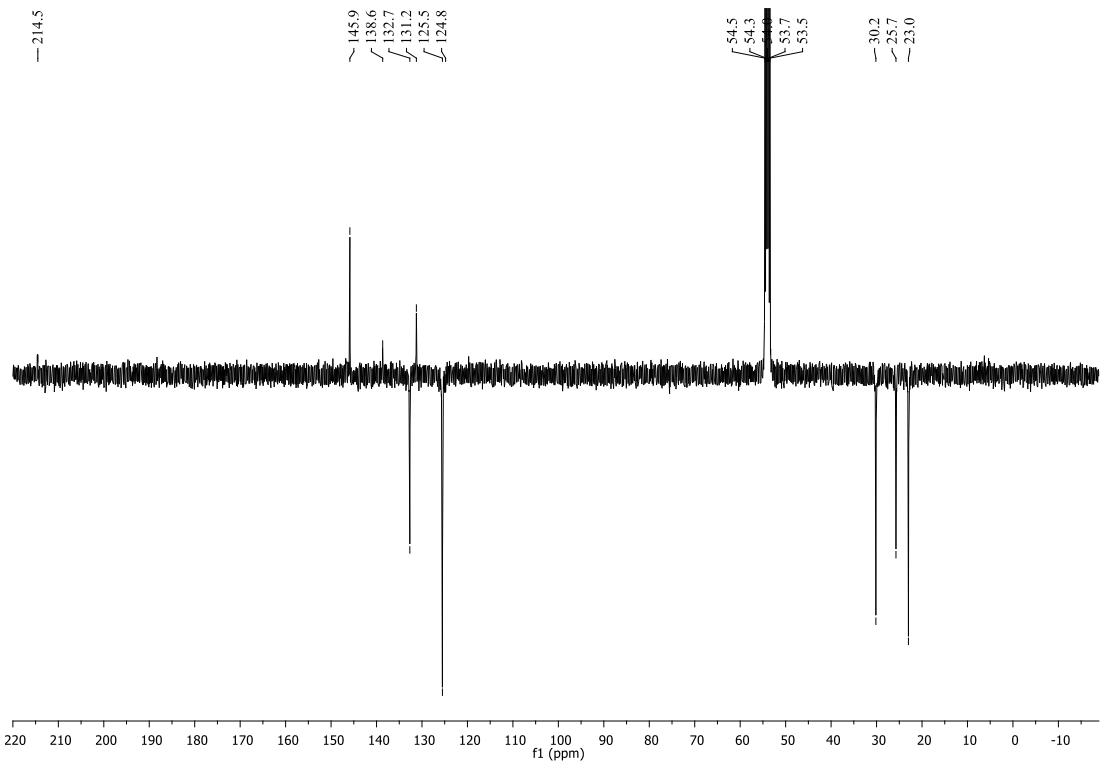

Figure S6. ^{13}C APT NMR spectrum (100 MHz, CD_2Cl_2, 298 K) of [MnBr(CO)$_3$(S$_2$C·IDip)] (**3**)

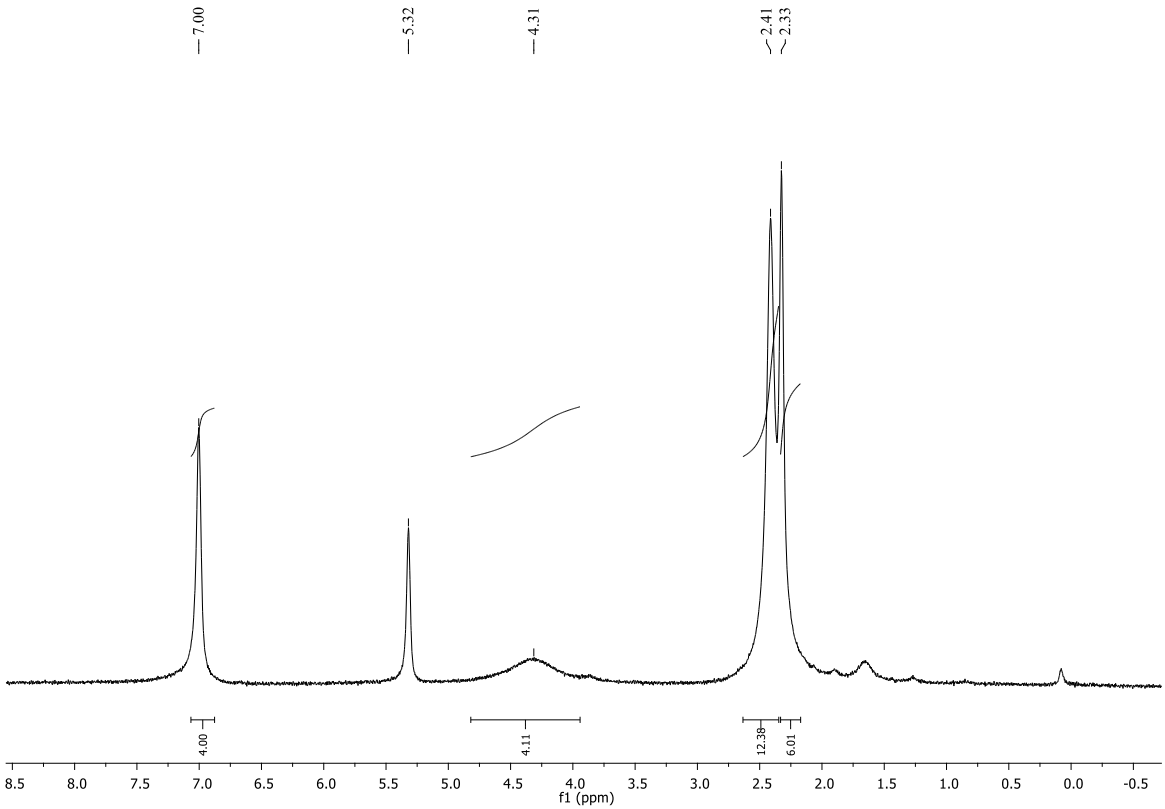

Figure S7. ^{1}H NMR spectrum (250 MHz, CD_2Cl_2, 298 K) of [MnBr(CO)$_3$(S$_2$C·SIMes)] (**4**)

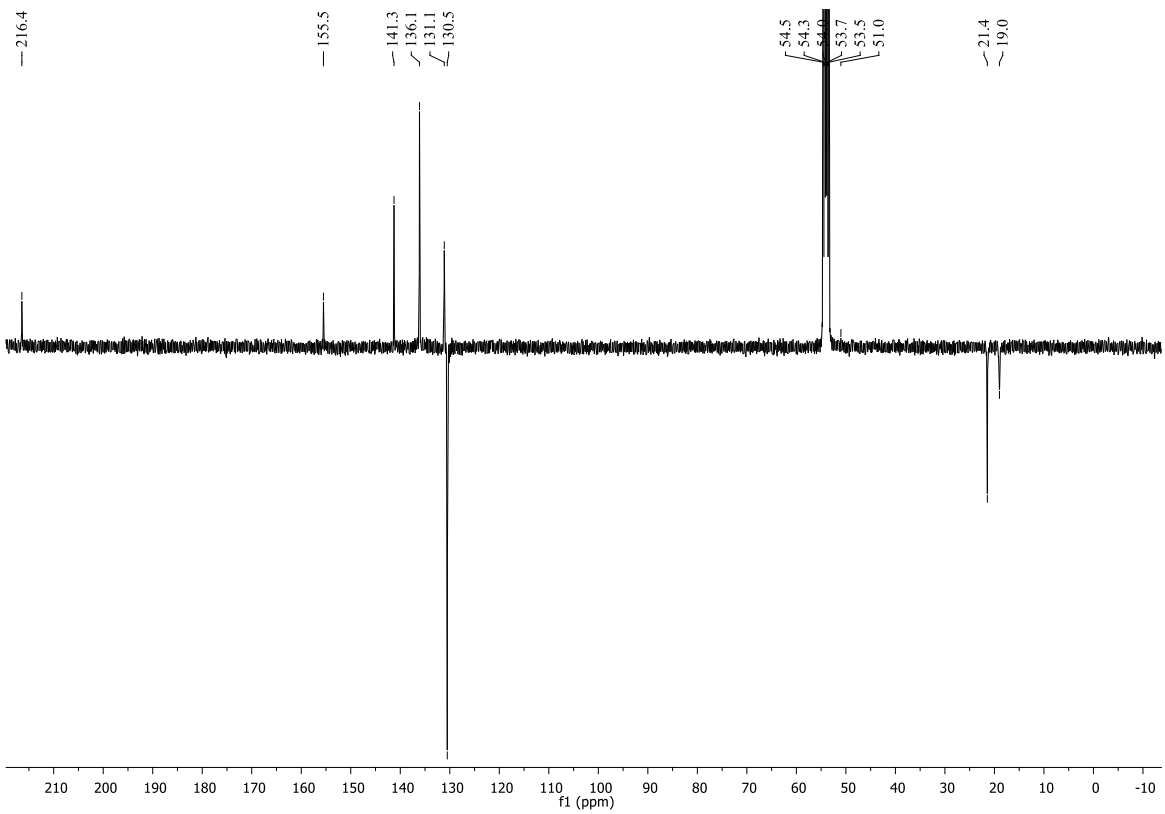

Figure S8. ^{13}C NMR spectrum (100 MHz, CD_2Cl_2, 298 K) of [MnBr(CO)$_3$(S$_2$C·SIMes)] (**4**)

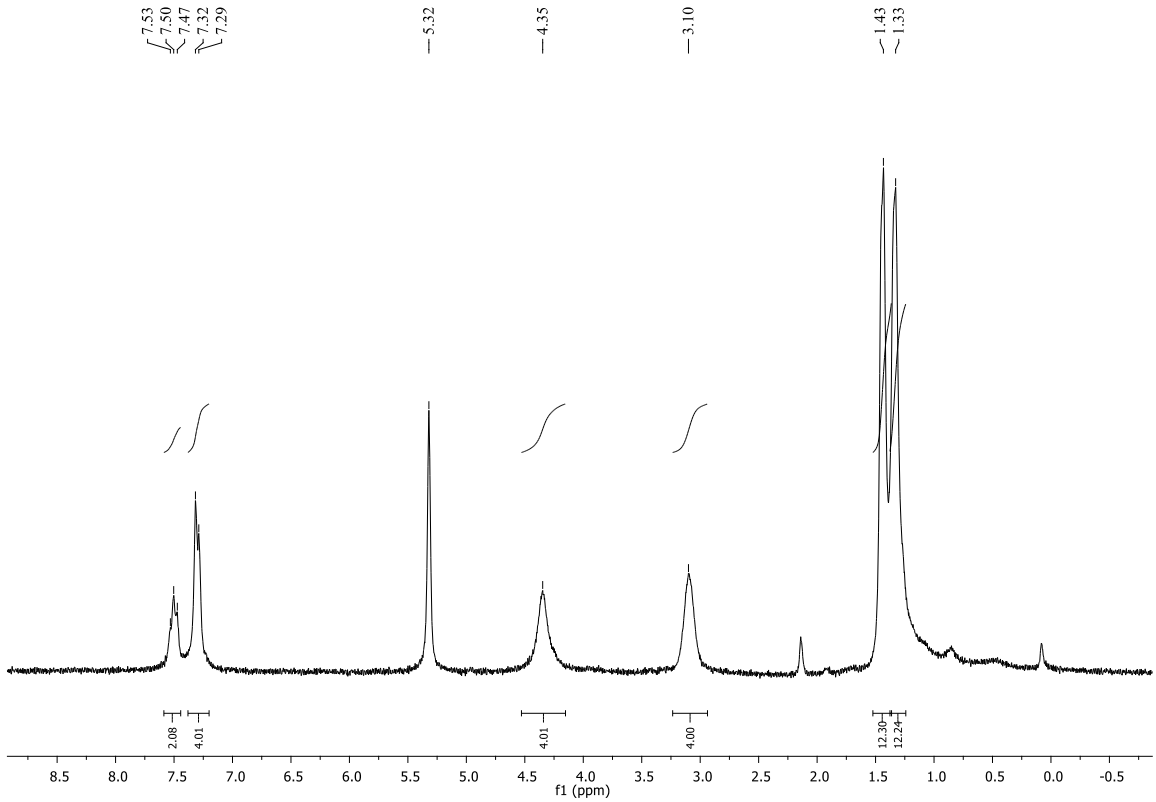

Figure S9. ^{1}H NMR spectrum (250 MHz, CD_2Cl_2, 298 K) of [MnBr(CO)$_3$(S$_2$C·SIDip)] (**5**)

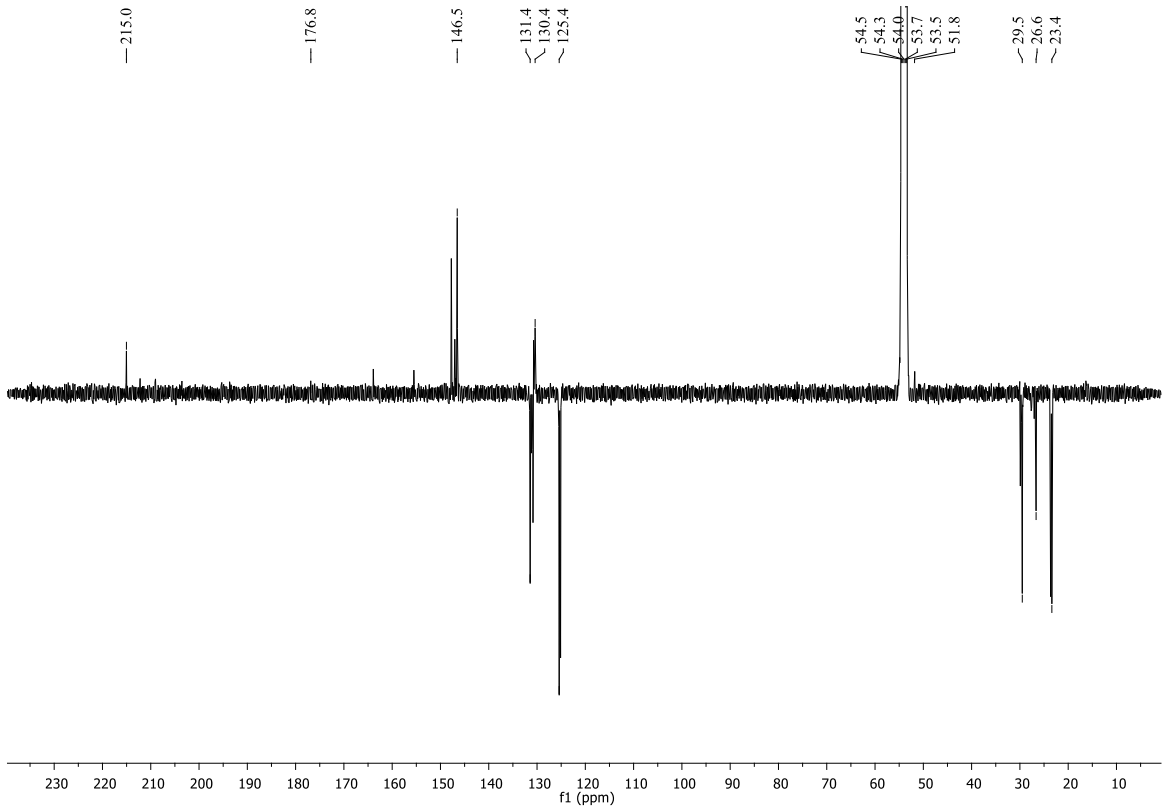

Figure S10. ^{13}C APT NMR spectrum (100 MHz, CD_2Cl_2, 298 K) of [MnBr(CO)$_3$(S$_2$C·SIDip)] (**5**)

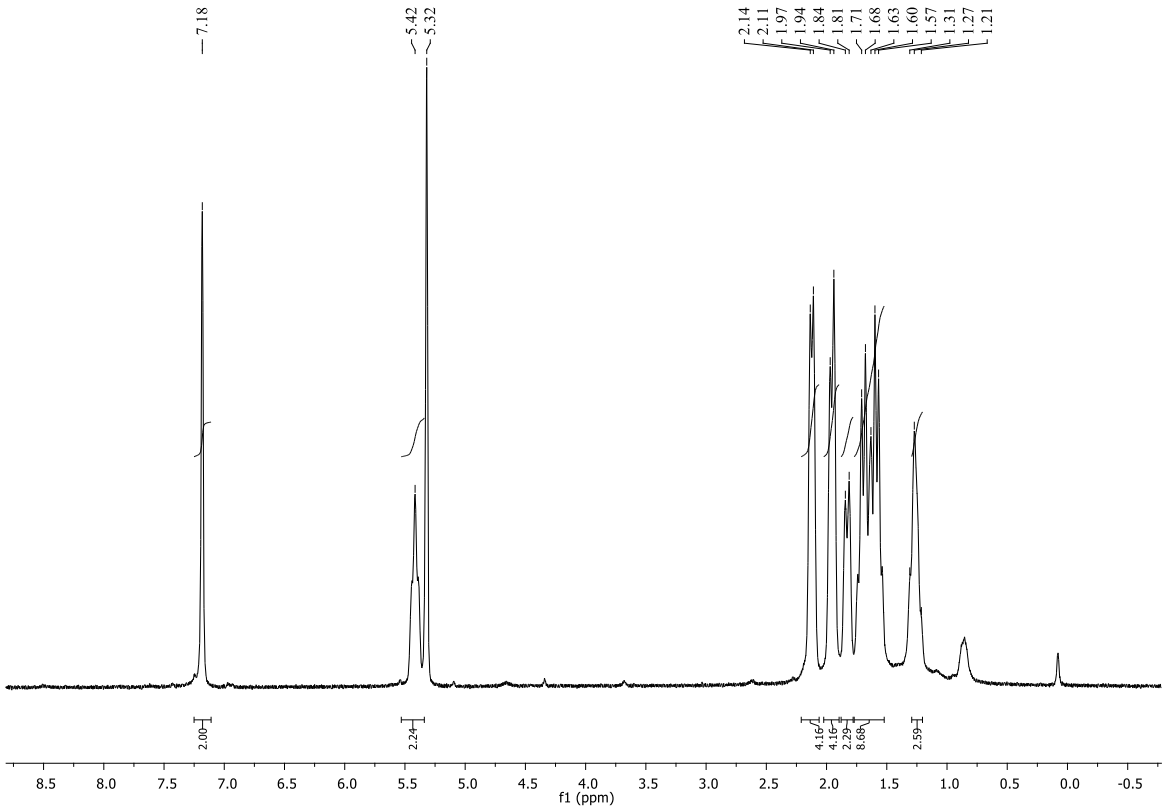

Figure S11. ^{1}H NMR spectrum (400 MHz, CD_2Cl_2, 298 K) of $[Mn_2(CO)_6(S_2C{\cdot}ICy)]$ (**6**)

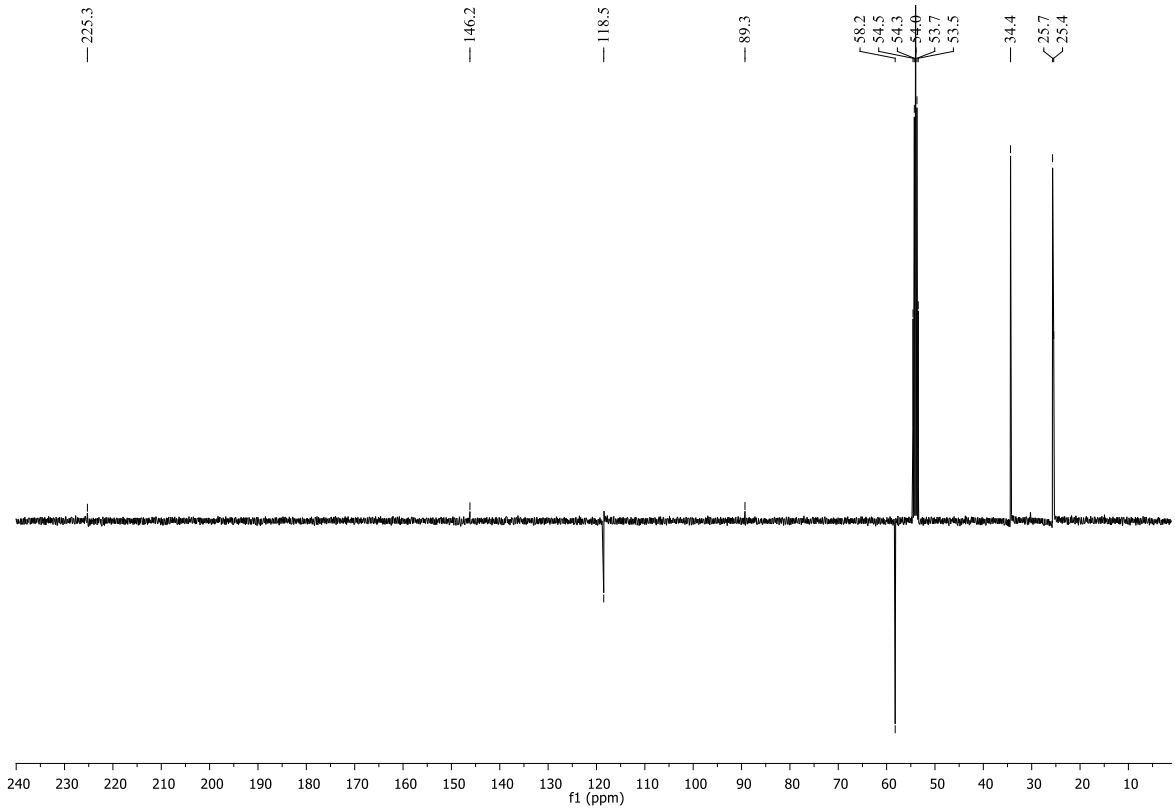

Figure S12. ^{13}C APT NMR spectrum (100 MHz, CD_2Cl_2, 298 K) of $[Mn_2(CO)_6(S_2C{\cdot}ICy)]$ (**6**)

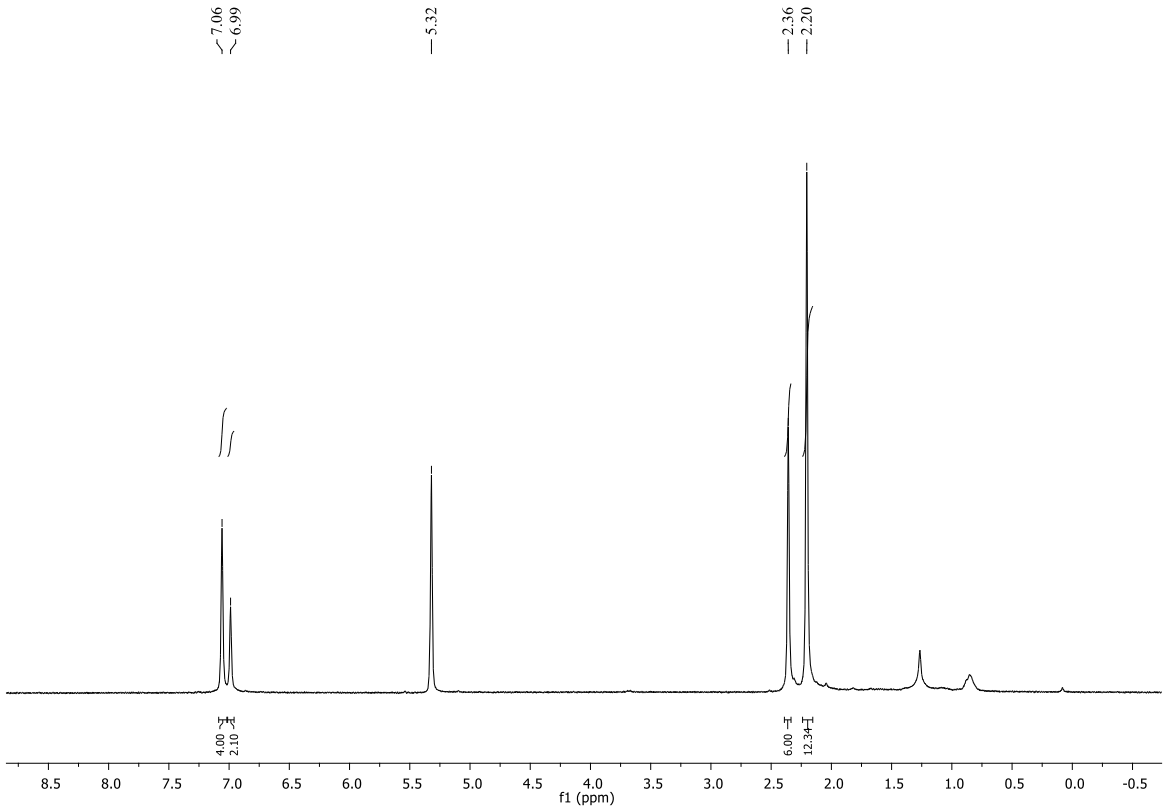

Figure S13. ^{1}H NMR spectrum (400 MHz, CD_2Cl_2, 298 K) of $[Mn_2(CO)_6(S_2C{\cdot}IMes)]$ (**7**)

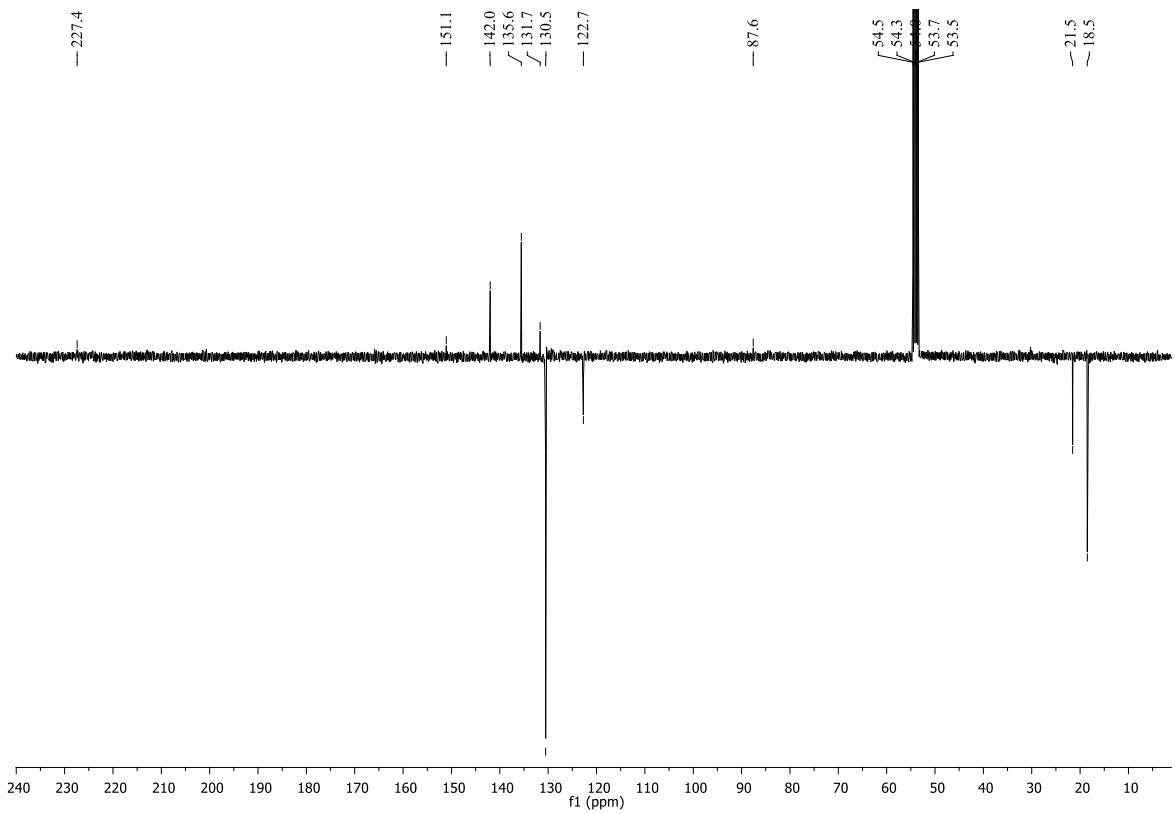

Figure S14. ^{13}C NMR spectrum (100 MHz, CD_2Cl_2, 298 K) of $[Mn_2(CO)_6(S_2C{\cdot}IMes)]$ (**7**)

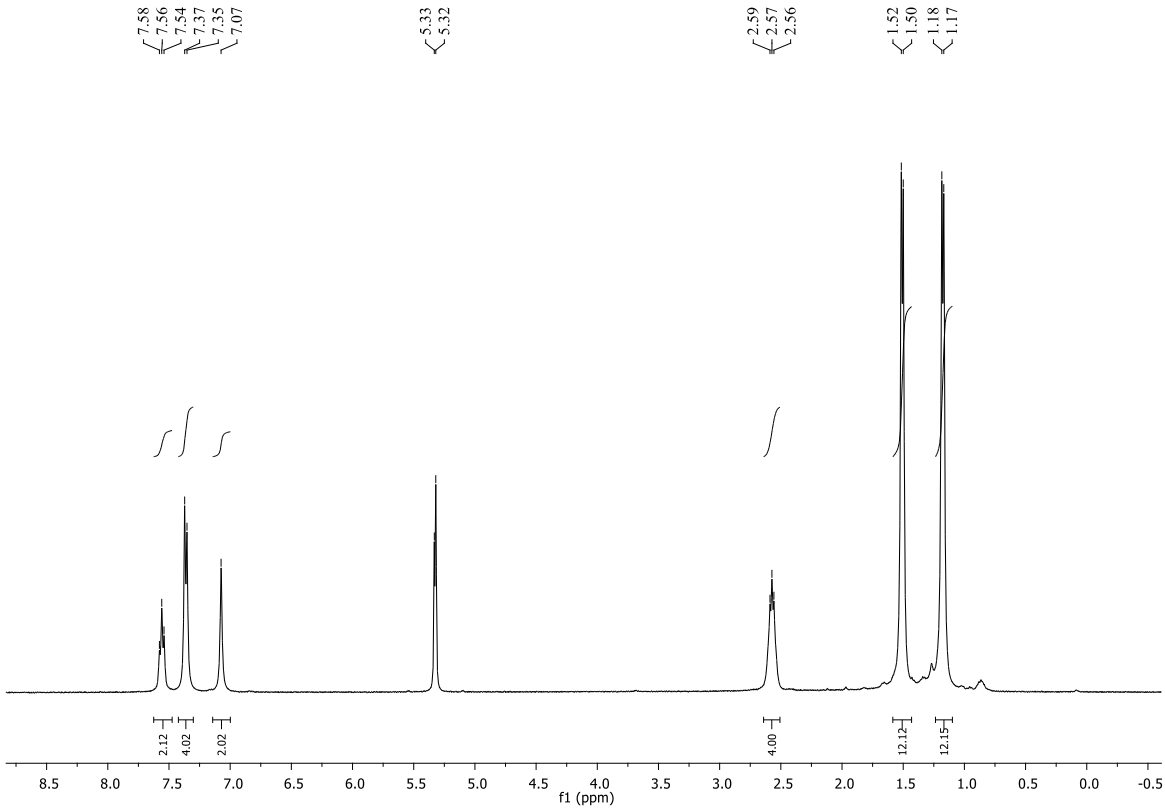

Figure S15. ^{1}H NMR spectrum (400 MHz,CD_2Cl_2, 298 K) of $[Mn_2(CO)_6(S_2C{\cdot}IDip)]$ (**8**)

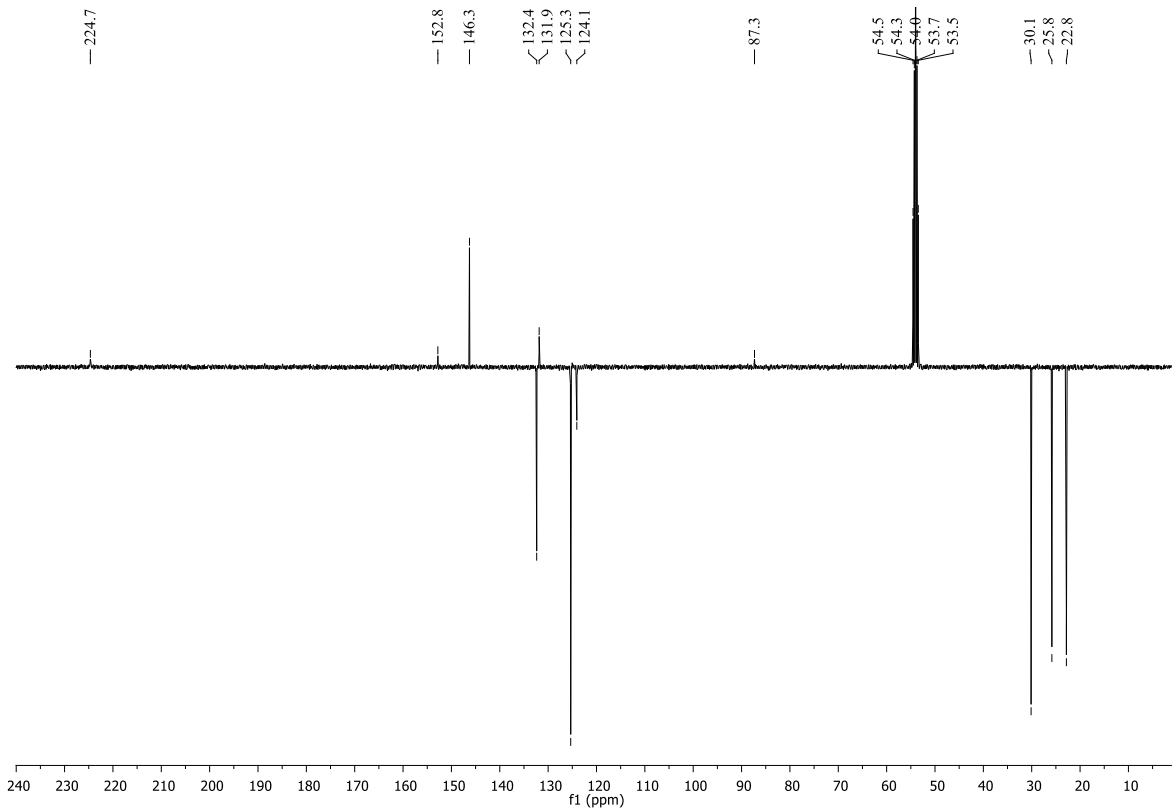

Figure S16. ^{13}C NMR spectrum (100 MHz, CD_2Cl_2, 273 K) of $[Mn_2(CO)_6(S_2C{\cdot}IDip)]$ (**8**)

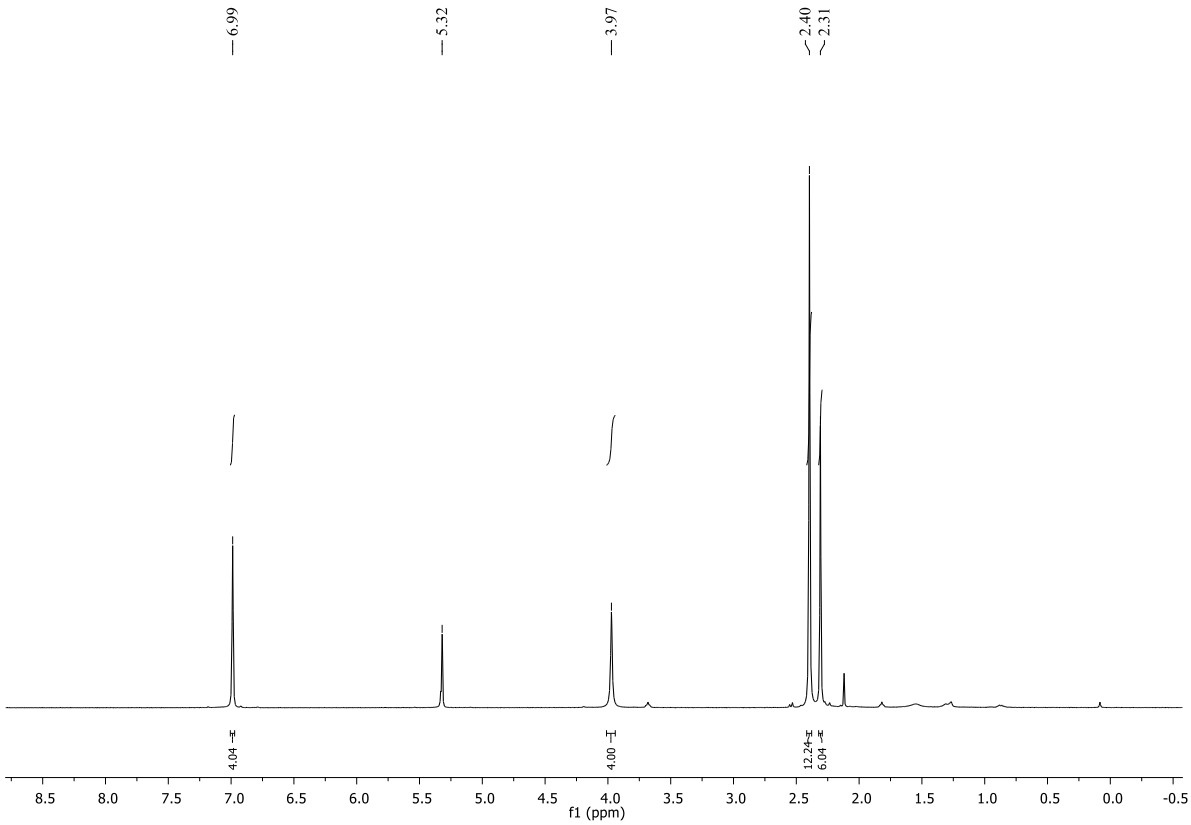

Figure S17. ^{1}H NMR spectrum (400 MHz, CD_2Cl_2, 298 K) of $[Mn_2(CO)_6(S_2C{\cdot}SIMes)]$ (**9**)

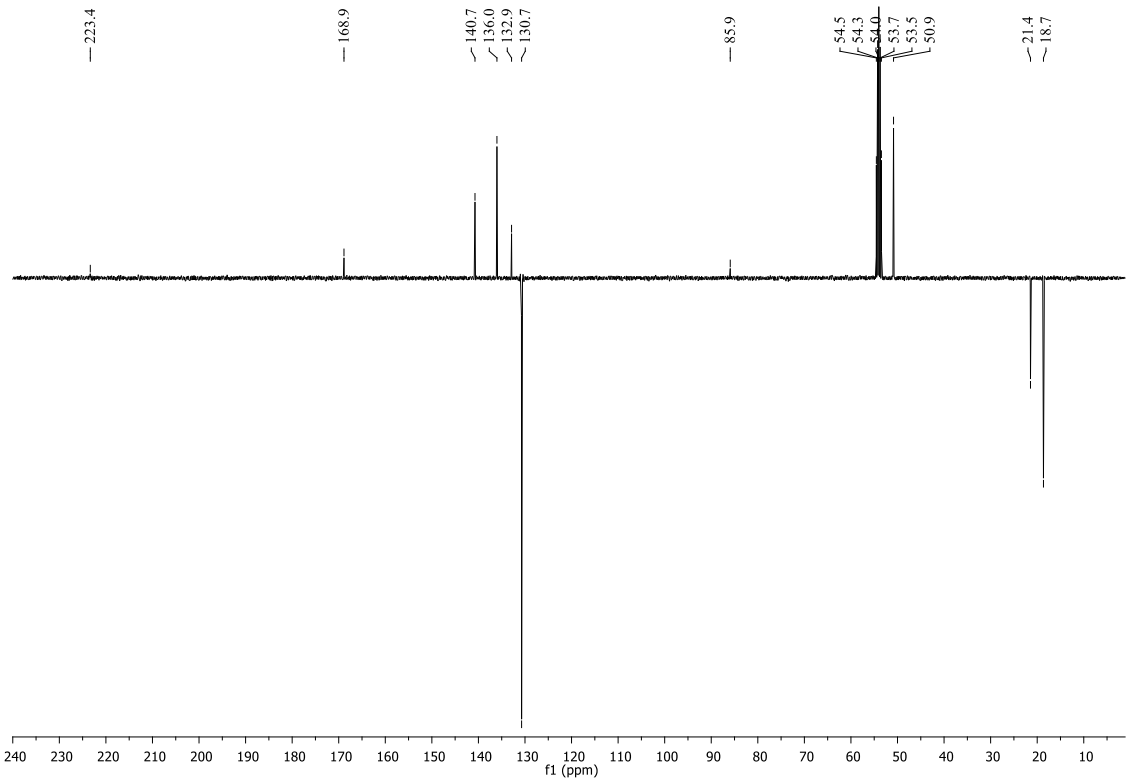

Figure S18. ^{13}C APT NMR spectrum (100 MHz, CD_2Cl_2, 298 K) of $[Mn_2(CO)_6(S_2C{\cdot}SIMes)]$ (**9**)

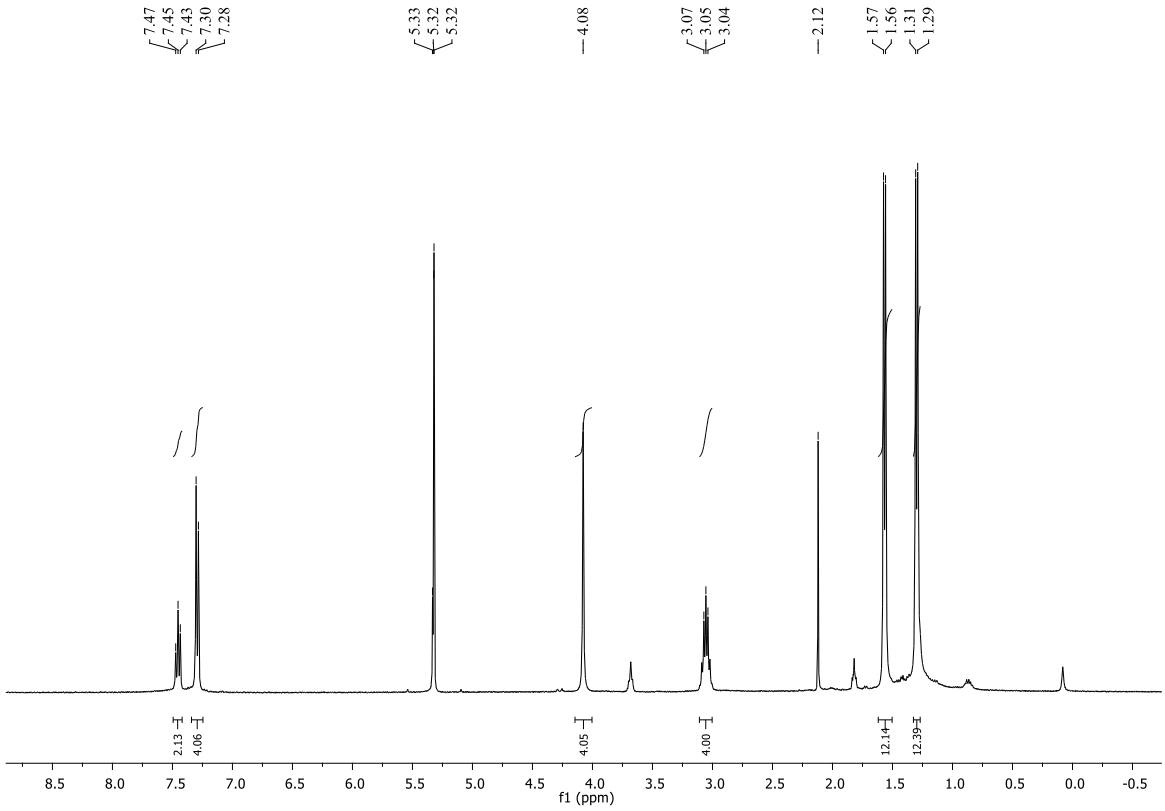

Figure S19. ^{1}H NMR spectrum (400 MHz, CD_2Cl_2, 298 K) of $[Mn_2(CO)_6(S_2C{\cdot}SIDip)]$ (**10**)

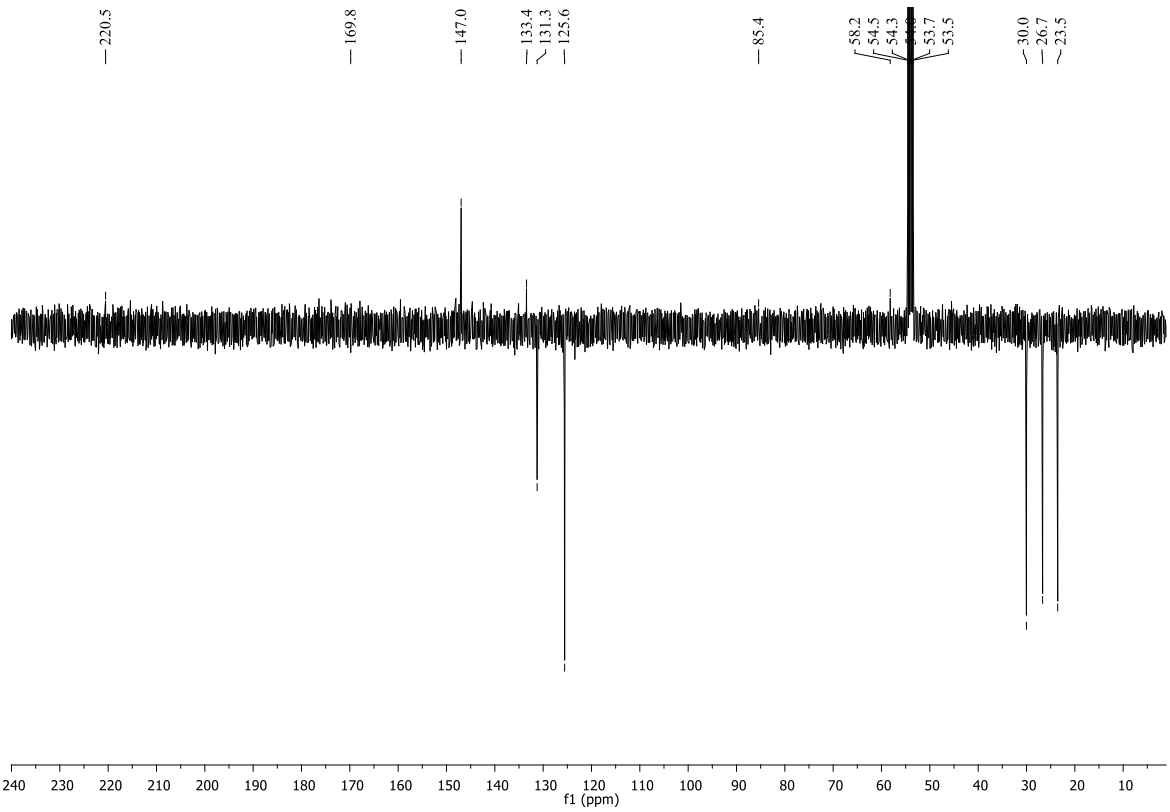

Figure S20. ^{13}C NMR spectrum (100 MHz, CD_2Cl_2, 298 K) of $[Mn_2(CO)_6(S_2C{\cdot}SIDip)]$ (**10**)

Part 3 – X-Ray Crystallography

1. General Information

X-Ray diffraction analyses were carried out on a Bruker APPEX II diffractometer using Mo-Kα radiation (λ = 0.71073 Å) from a fine focus sealed tube source at 100 K. Computing data and reduction was made with the APPEX II software.[2] No instrument or crystal instabilities were observed during data collection. Absorption corrections based on the multiscan method were applied.[3] All the structures were solved using SIR2004.[4] They were refined by full-matrix, least-squares based on F^2 using SHELXL.[5] An empirical absorption correction was applied using SADABS.[6] All non-hydrogen atoms were anisotropically refined and the hydrogen atom positions were calculated and refined using a riding model. The ORTEP representations were drawn using the Diamond visual crystal structure information system software.[7]

2. Crystal Data for Complexes 3–6 and 8–10

CCDC 1523424–1523430 contain the supplementary crystallographic data (excluding structure factors) for the structures reported in this paper. These data can be obtained free of charge from The Cambridge Crystallographic Data Centre via https://summary.ccdc.cam.ac.uk/structure-summary-form or on application to CCDC, 12 Union Road, Cambridge CB2 1EZ, UK [fax.: (internat.) +44–1223/336–033].

[MnBr(CO)$_3$(S$_2$C·IDip)] (3). Blue-green crystals with dimensions 0.20 × 0.17 × 0.04 mm obtained by slow diffusion of *n*-hexane into a CH_2Cl_2 solution at –20 °C. $C_{31}H_{36}BrMnN_2O_3S_2$ M = 683.6, orthorhombic, space group *Pbcn*, a = 10.3812(5) Å, b = 19.7434(8) Å, c = 15.7821(7) Å, α = 90°, β = 90°, γ = 90°, V = 3234.7(2) Å^3, T = 100(2) K, Z = 4, μ (Mo Kα) = 1.805 mm^{-1}. Reflections collected/unique = 13533/1978 (R_{int} = 0.0789). Final refinement converged with R_1 = 0.0935 and wR_2 = 0.1465 for all reflections, GOF = 1.020, max/min residual electron density 0.36 /–0.35 e·Å^{-3}.

[MnBr(CO)$_3$(S$_2$C·SIMes)] (4). Blue-green crystals with dimensions 0.15 × 0.12 × 0.02 mm obtained by slow diffusion of diethylether into a CH_2Cl_2 solution at –20 °C. $C_{25}H_{26}BrMnN_2O_3S_2$, M = 601.45, monoclinic, space group $P2_1/c$, a = 16.2293(11) Å, b = 10.2810(7) Å, c = 16.2491(12) Å, α = 90°, β = 104.615(2)°, γ = 90°, V = 2623.5(3) Å^3, T = 100(2) K, Z = 4, μ (Mo Kα) = 2.215 mm^{-1}. Reflections collected/unique = 14586/4788 (R_{int} = 0.0771). Final refinement

converged with R_1 = 0.1123 and wR_2 = 0.1229 for all reflections, GOF = 1.010, max/min residual electron density 0.91/–0.53 e·Å^{-3}.

[MnBr(CO)$_3$(S$_2$C·SIDip)]$_2$·3 CH$_2$Cl$_2$ (5). Blue-green crystals with dimensions 0.20 × 0.13 × 0.09 mm obtained by slow diffusion of *n*-hexane into a CH_2Cl_2 solution at 6 °C. $C_{65}H_{82}Br_2Cl_6Mn_2N_4O_6S_4$ M = 1625.97, monoclinic, space group $P2_1/n$, a = 11.5907(13) Å, b = 17.763(2) Å, c = 17.955(2) Å, α = 90°, β = 91.522(10)°, γ = 90°, V = 3695.4(8) Å^3, T = 100(2) K, Z = 2, μ (Mo Kα) = 1.803 mm^{-1}. Reflections collected/unique = 68581/9178 (R_{int} = 0.0532). Final refinement converged with R_1 = 0.0501 and wR_2 = 0.0880 for all reflections, GOF = 1.019, max/min residual electron density 0.63/–0.65 e·Å^{-3}.

[Mn$_2$(CO)$_6$(S$_2$C·ICy)] (6). Orange crystals with dimensions 0.32 × 0.20 × 0.15 mm obtained by slow diffusion of *n*-hexane into a CH_2Cl_2 solution at 6 °C. $C_{22}H_{24}Mn_2N_2O_6S_2$ M = 586.43, triclinic, space group $P\text{–}1$, a = 11.1085(4) Å, b = 11.6937(4) Å, c = 12.1298(4) Å, α = 69.906(2)°, β = 63.919(2)°, γ = 62.296(2)°, V = 1233.64(8) Å^3, T = 100(2) K, Z = 2, μ (Mo Kα) = 1.233 mm^{-1}. Reflections collected/unique = 56201/7212 (R_{int} = 0.0231). Final refinement converged with R_1 = 0.0231 and wR_2 = 0.0505 for all reflections, GOF = 1.039, max/min residual electron density 0.38/–0.28 e·Å^{-3}.

[Mn$_2$(CO)$_6$(S$_2$C·IDip)]$_2$·CH$_2$Cl$_2$ (8). Red crystals with dimensions 0.35 × 0.28 × 0.17 mm obtained by slow diffusion of *n*-hexane into a CH_2Cl_2 solution at 6 °C. $C_{69}H_{74}Cl_2Mn_4N_4O_{12}S_4$ M = 1570.22, orthorhombic, space group $Aba2$, a = 38.0525(12) Å, b = 11.4280(4) Å, c = 16.6104(6) Å, α = 90°, β = 90°, γ = 90°, V = 7223.3(4) Å^3, T = 100(2) K, Z = 4, μ (Mo Kα) = 0.934 mm^{-1}. Reflections collected/unique = 45708/9939 (R_{int} = 0.0571). Final refinement converged with R_1 = 0.0475 and wR_2 = 0.0721 for all reflections, GOF = 0.982, max/min residual electron density 0.34/–0.32 e·Å^{-3}.

[Mn$_2$(CO)$_6$(S$_2$C·SIMes)] (9). Red crystals with dimensions 0.26 × 0.16 × 0.09 mm obtained by slow diffusion of *n*-hexane into a CH_2Cl_2 solution at 6 °C. $C_{28}H_{26}Mn_2N_2O_6S_2$ M = 660.51, monoclinic, space group $P2_1/n$, a = 14.5947(4) Å, b = 10.6565(3) Å, c = 18.7588(6) Å, α = 90°, β = 97.837(2)°, γ = 90°, V = 2890.28(15) Å^3, T = 100(2) K, Z = 4, μ (Mo Kα) = 1.062 mm^{-1}. Reflections collected/unique = 65200/8814 (R_{int} = 0.0446). Final refinement converged with R_1 = 0.0485 and wR_2 = 0.0698 for all reflections, GOF = 1.028, max/min residual electron density 0.48/–0.32 e·Å^{-3}.

[Mn$_2$(CO)$_6$(S$_2$C·SIDip)]$_2$·CH$_2$Cl$_2$ (10). Red crystals with dimensions 0.20 × 0.13 × 0.09 mm obtained by slow diffusion of *n*-hexane into a CH_2Cl_2 solution at 6 °C. $C_{69}H_{78}Cl_2Mn_4N_4O_{12}S_4$ M = 1574.25, orthorhombic, space group $Aba2$, a = 38.3937(13) Å, b = 11.4255(4) Å, c = 16.4614(6)

Å, $\alpha = 90°$, $\beta = 90°$, $\gamma = 90°$, $V = 7221.1(4)$ Å^3, $T = 100(2)$ K, $Z = 4$, μ (Mo Kα) = 0.935 mm^{-1}. Reflections collected/unique = 49103/8930 ($R_{int} = 0.0539$). Final refinement converged with R_1 = 0.0479 and wR_2 = 0.0819 for all reflections, GOF = 1.020, max/min residual electron density 0.45/–0.50 e·Å^{-3}.

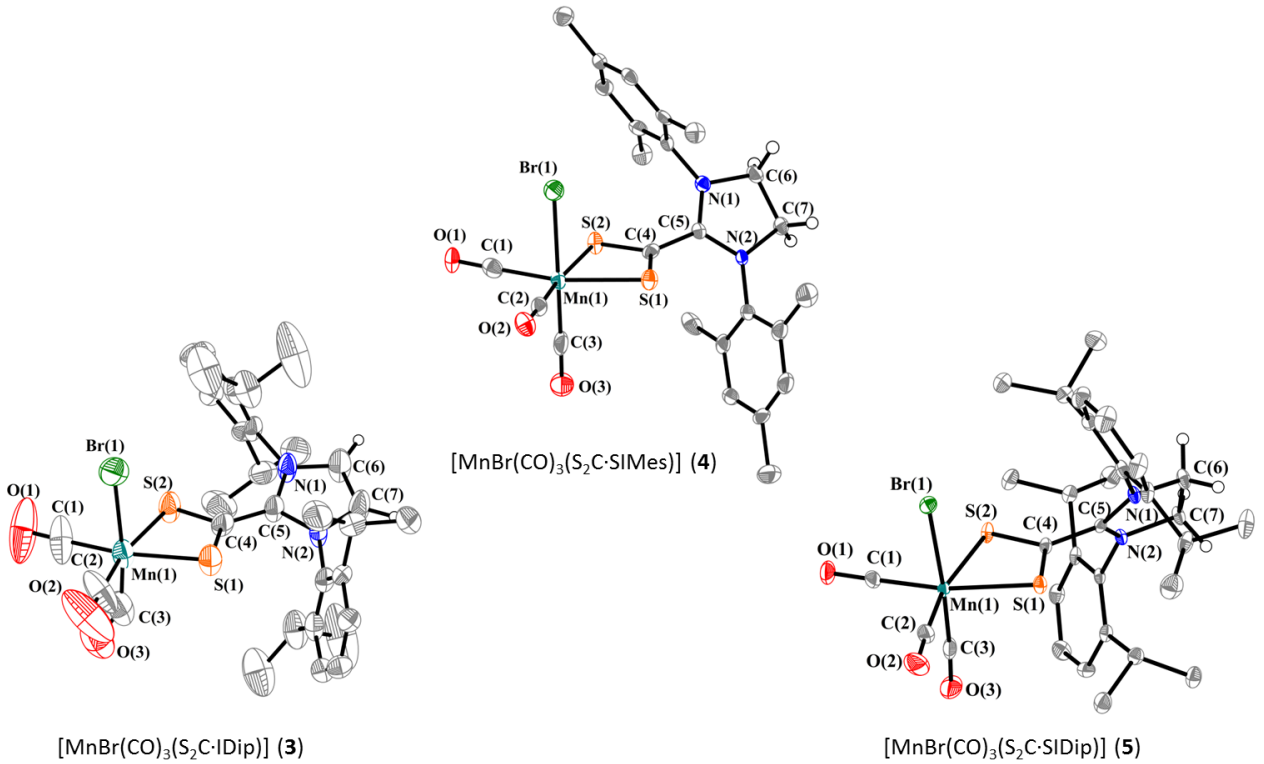

Figure S21. ORTEP representations of [MnBr(CO)$_3$(S$_2$C·IDip)] (**3**), [MnBr(CO)$_3$(S$_2$C·SIMes)] (**4**), and [MnBr(CO)$_3$(S$_2$C·SIDip)] (**5**) (ellipsoids drawn at the 50% probability level). Co-crystallized solvent molecules and hydrogen atoms were omitted, except those directly bonded to the heterocyclic ring in order to emphasize the presence or the absence of a double bond

Table S1. Selected Bond Distances (Å) and Angles (deg) Derived from the Molecular Structures of Complexes **3**, **4**, and **5**[a]

Complex	**3**[b]	**4**	**5**
Mn–C(1)	1.801(8)	1.822(6)	1.803(2)
Mn–C(2)	1.801(8)	1.800(7)	1.811(3)
Mn–C(3)	1.82(3)	1.789(6)	1.796(2)
Mn–S(1)	2.3639(18)	2.4099(16)	2.3901(7)
Mn–S(2)	2.3639(18)	2.3585(17)	2.4005(7)
Mn–Br(1)	2.574(2)	2.5350(10)	2.5278(5)
C(4)–S(1)	1.681(4)	1.666(5)	1.670(2)
C(4)–S(2)	1.681(4)	1.667(5)	1.671(2)
C(4)–C(5)	1.464(10)	1.487(7)	1.481(3)
N(1)–C(5)	1.347(6)	1.316(6)	1.323(3)
N(2)–C(5)	1.347(6)	1.327(6)	1.324(3)
C(6)–C(7)	1.360(12)	1.524(7)	1.532(3)
C(1)–Mn(1)–C(2)	97.4(5)	93.1(2)	94.42(11)
C(1)–Mn(1)–C(3)	83.4(6)	95.0(3)	90.32(10)
C(2)–Mn(1)–C(3)	91.2(7)	89.5(3)	89.34(11)
C(1)–Mn(1)–S(1)	167.8(3)	166.89(18)	169.67(8)
C(1)–Mn(1)–S(2)	94.8(3)	94.95(19)	98.17(8)
C(1)–Mn(1)–Br(1)	88.7(3)	84.62(18)	86.16(7)
S(1)–Mn(1)–S(2)	73.04(8)	73.09(5)	72.964(19)
S(1)–C(4)–S(2)	113.7(4)	116.9(3)	116.99(12)
N(1)–C(5)–C(4)–S(1)	–155.5(3)	–128.3(5)	–57.6(3)
N(2)–C(5)–C(4)–S(1)	24.5(3)	51.8(7)	121.66(19)

[a]See Figure S21 for atom labeling.

[b]C(2), N(2), S(2), C(7) → $C(1)^i$, $S(1)^i$, $N(1)^i$, $C(6)^i$; i = Symm (1–x, y, 0.5–z)

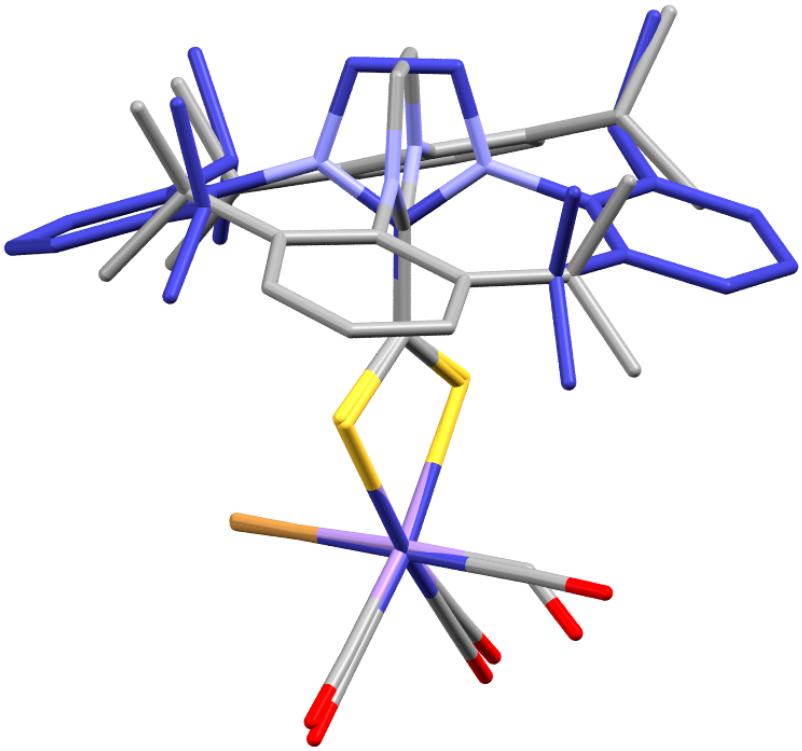

Figure S22. Superimposition of the molecular structures of [MnBr(CO)$_3$(S$_2$C·IDip)] (**3**) (grey) and [ReBr(CO)$_3$(S$_2$C·IDip)][8] (blue)

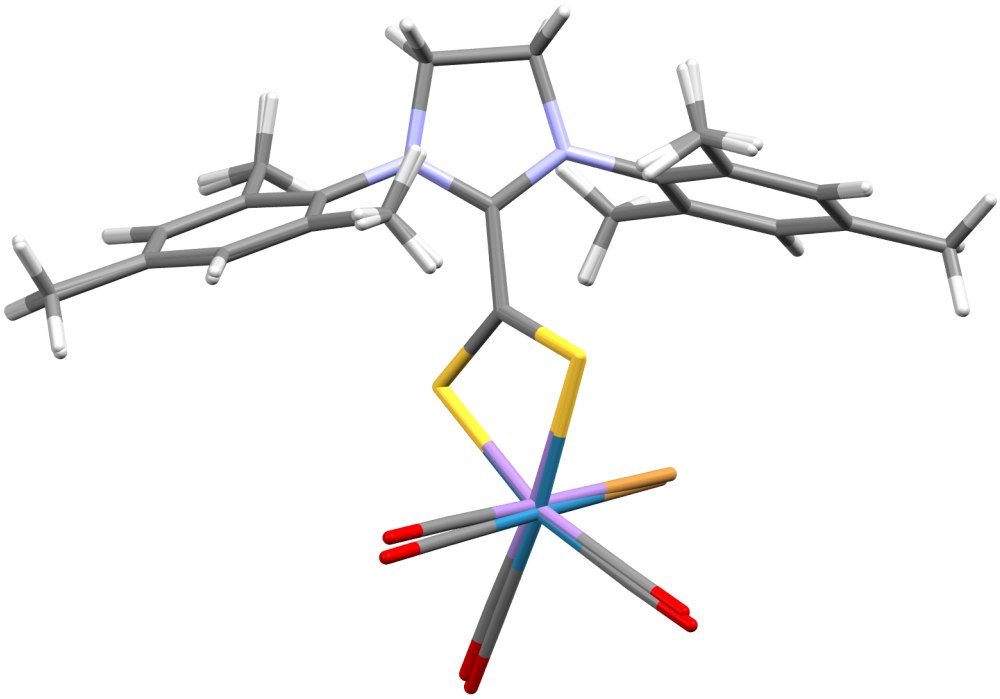

Figure S23. Superimposition of the molecular structures of [MnBr(CO)$_3$(S$_2$C·SIMes)] (**4**) and [ReBr(CO)$_3$(S$_2$C·SIMes)][8] (isostructural compounds)

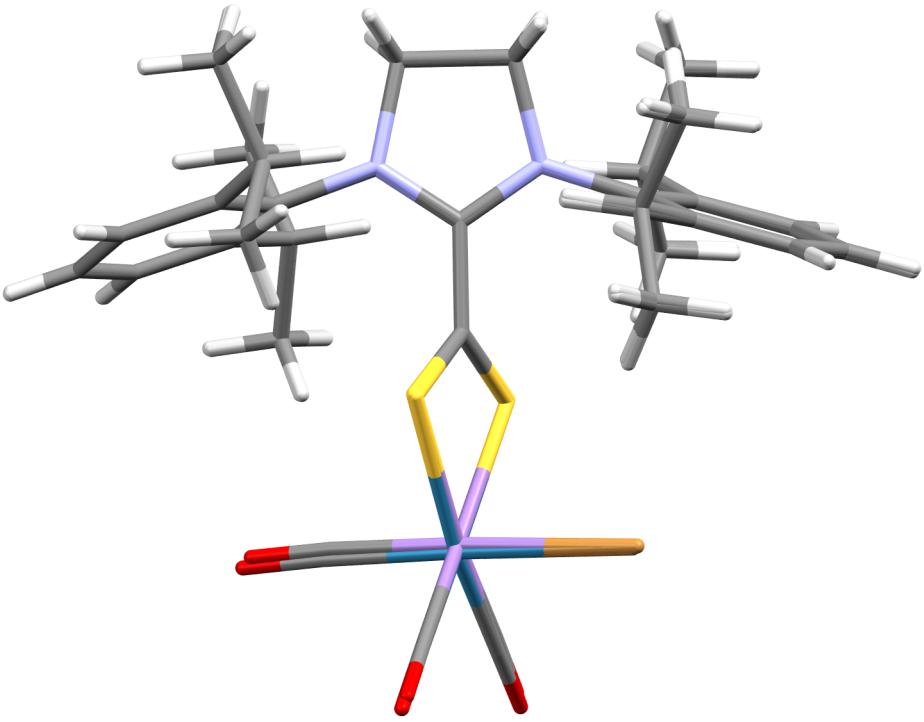

Figure S24. Superimposition of the molecular structures of [MnBr(CO)$_3$(S$_2$C·SIDip)] (**5**) and [ReBr(CO)$_3$(S$_2$C·SDip)][8] (isostructural compounds)

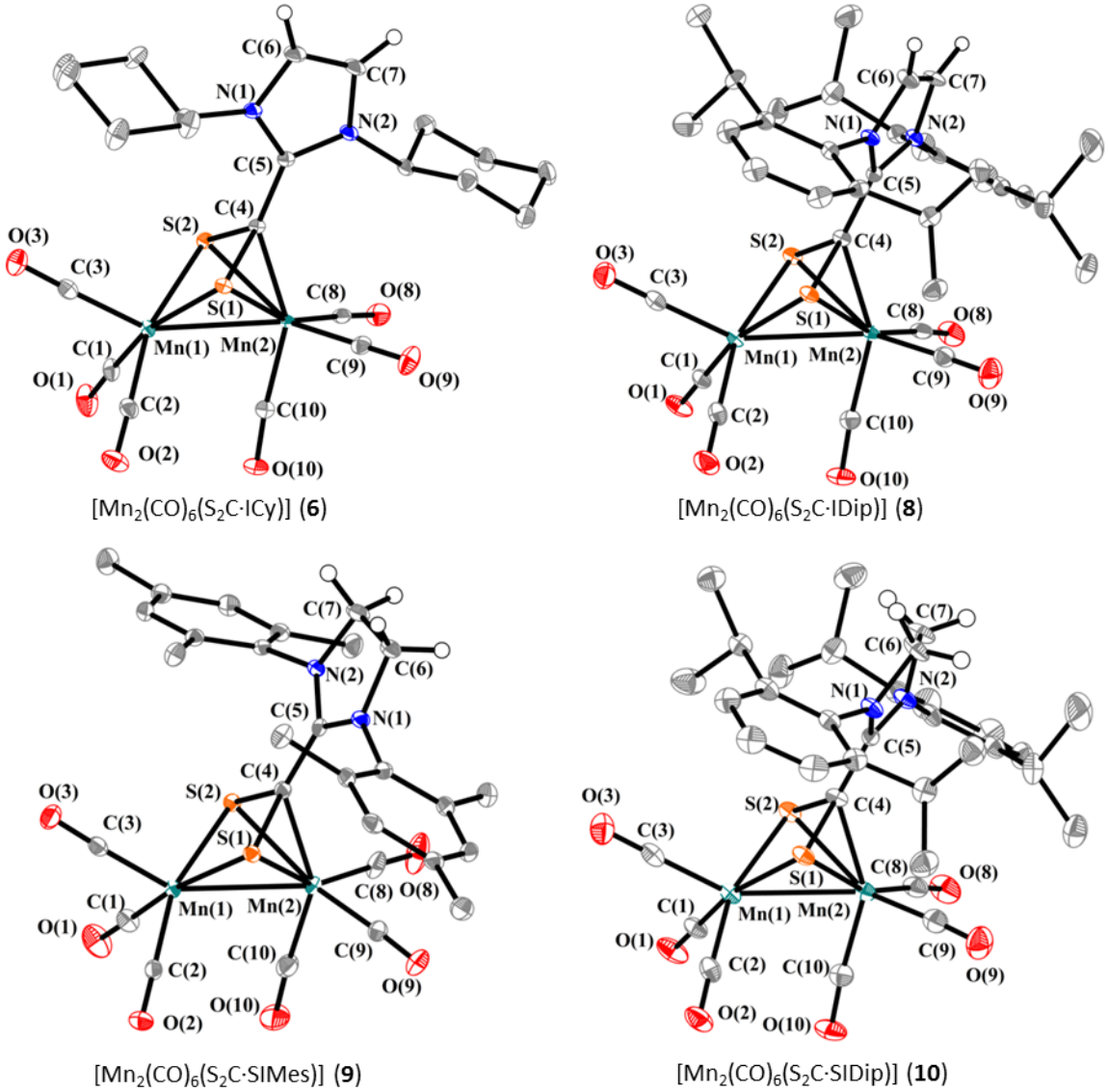

Figure S25. ORTEP representations of $[Mn_2(CO)_6(S_2C{\cdot}ICy)]$ (**6**), $[Mn_2(CO)_6(S_2C{\cdot}IDip)]$ (**8**), $[Mn_2(CO)_6(S_2C{\cdot}SIMes)]$ (**9**), and $[Mn_2(CO)_6(S_2C{\cdot}SIDip)]$ (**10**) (ellipsoids drawn at the 50% probability level). Co-crystallized solvent molecules and hydrogen atoms were omitted, except those directly bonded to the heterocyclic ring in order to emphasize the presence or the absence of a double bond

Table S2. Selected Bond Distances (Å) and Angles (deg) Derived from the Molecular Structures of Complexes **6**, **8**–**10**[a]

Complex	**6**	**8**	**9**	**10**
Mn(1)–Mn(2)	2.6992(2)	2.6957(6)	2.7320(3)	2.7003(8)
Mn(1)–C(1)	1.8156(11)	1.800(3)	1.8256(17)	1.802(4)
Mn(1)–C(2)	1.8111(11)	1.809(3)	1.8148(16)	1.809(4)
Mn(1)–C(3)	1.7819(11)	1.785(3)	1.7669(16)	1.774(5)
Mn(2)–C(8)	1.7974(11)	1.810(3)	1.8006(17)	1.810(4)
Mn(2)–C(9)	1.8049(11)	1.809(3)	1.8006(17)	1.809(5)
Mn(2)–C(10)	1.7972(10)	1.791(3)	1.8044(17)	1.791(4)
Mn(1)–S(1)	2.2768(3)	2.2778(8)	2.2602(4)	2.2763(11)
Mn(1)–S(2)	2.2937(3)	2.2784(8)	2.2697(4)	2.2764(10)
Mn(2)–S(1)	2.3293(3)	2.3418(8)	2.3127(4)	2.3340(11)
Mn(2)–S(2)	2.3408(3)	2.3199(8)	2.3340(4)	2.3191(11)
Mn(2)–C(4)	2.0345(9)	2.064(3)	2.0715(14)	2.081(4)
S(1)–C(4)	1.7725(10)	1.767(3)	1.7668(15)	1.767(4)
S(2)–C(4)	1.7759(10)	1.775(3)	1.7678(15)	1.773(4)
C(4)–C(5)	1.4599(13)	1.440(4)	1.436(2)	1.428(5)
N(1)–C(5)	1.3531(13)	1.363(3)	1.3374(19)	1.349(4)
N(2)–C(5)	1.3480(13)	1.355(3)	1.3429(19)	1.335(5)
C(6)–C(7)	1.3491(16)	1.340(4)	1.524(2)	1.507(5)
C(1)–Mn(1)–S(1)	162.95(3)	162.07(10)	165.89(5)	162.57(13)
C(1)–Mn(1)–S(2)	97.13(4)	95.14(9)	95.92(5)	94.59(12)
C(1)–Mn(1)–Mn(2)	108.05(3)	106.67(9)	111.69(5)	107.42(13)
C(8)–Mn(2)–S(1)	159.54(3)	159.35(9)	150.03(6)	159.29(13)
C(8)–Mn(2)–S(2)	95.34(3)	92.92(10)	95.26(6)	92.54(14)
C(8)–Mn(2)–Mn(1)	132.86(3)	129.86(10)	139.75(5)	129.62(14)
C(8)–Mn(2)–C(4)	112.57(4)	112.63(12)	105.07(7)	112.59(16)
S(1)–C(4)–S(2)	103.78(5)	103.74(14)	103.98(8)	103.94(19)
Mn(1)–S(1)–C(4)–S(2)	2.86(4)	1.22(12)	–1.61(6)	–0.31(17)
N(1)–C(5)–C(4)–S(1)	–54.4(2)	–18.5(4)	29.4(2)	–12.9(6)
N(2)–C(5)–C(4)–S(1)	125.91(10)	162.1(2)	–149.89(12)	168.3(3)

[a]See Figure S25 for atom labeling.

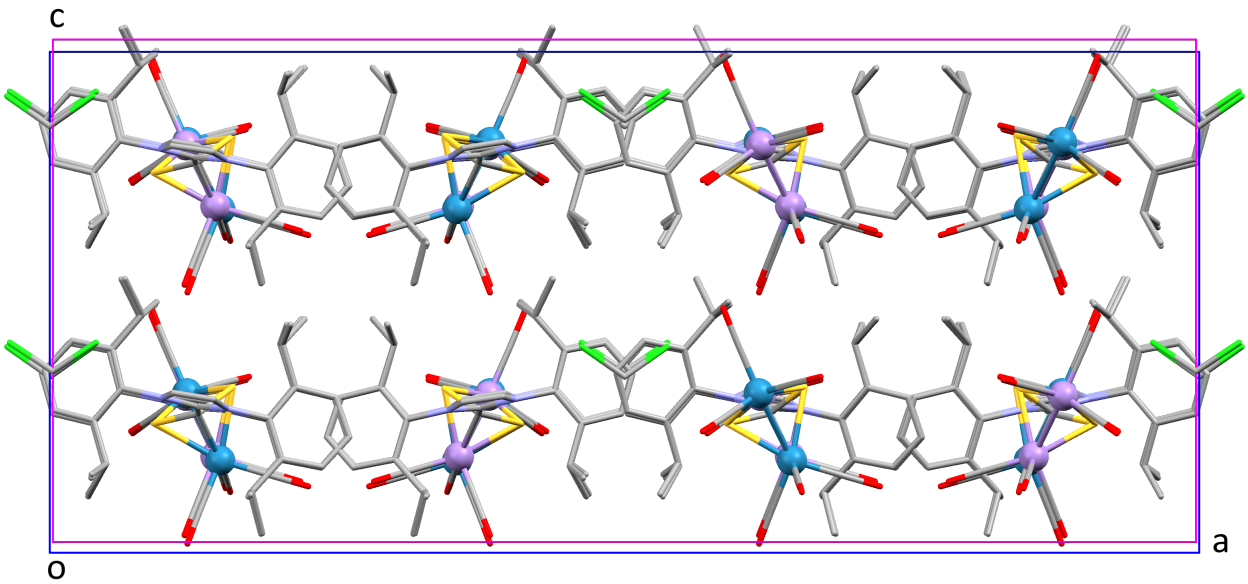

Figure S26. Superimposition of isostructural unit cells for $[Mn_2(CO)_6(S_2C{\cdot}IDip)]_2{\cdot}CH_2Cl_2$ (**8**) and $[Re_2(CO)_6(S_2C{\cdot}IDip)]_2{\cdot}CH_2Cl_2$[8]

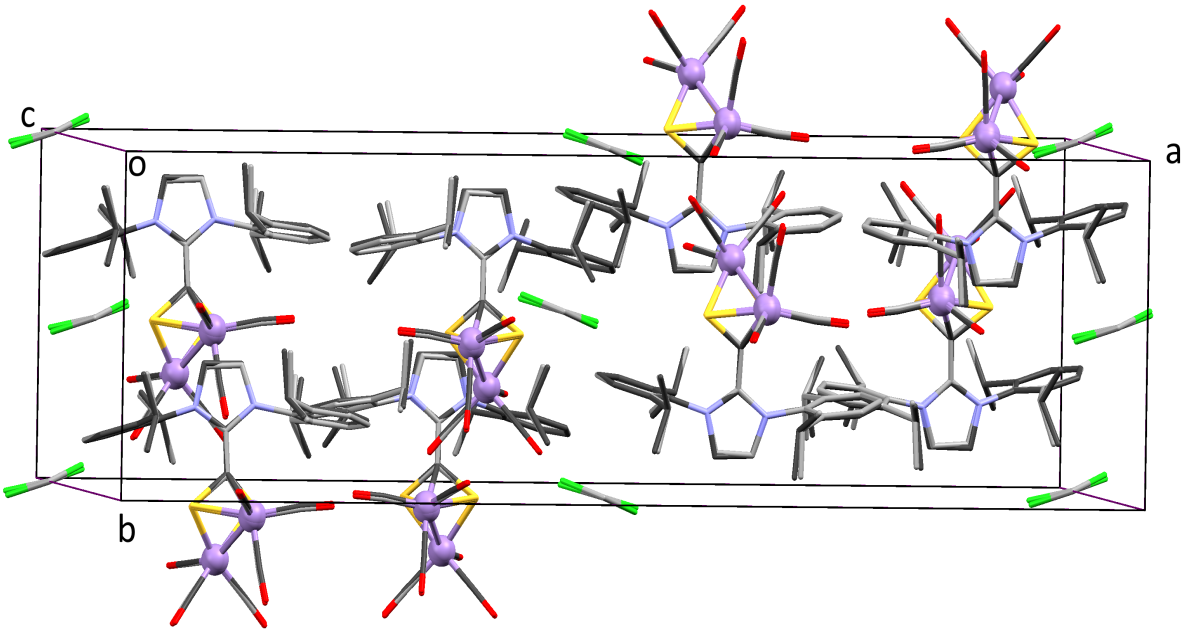

Figure S27. Superimposition of isostructural unit cells for $[Mn_2(CO)_6(S_2C{\cdot}IDip)]_2{\cdot}CH_2Cl_2$ (**8**) and $[Mn_2(CO)_6(S_2C{\cdot}SIDip)]_2{\cdot}CH_2Cl_2$ (**10**)

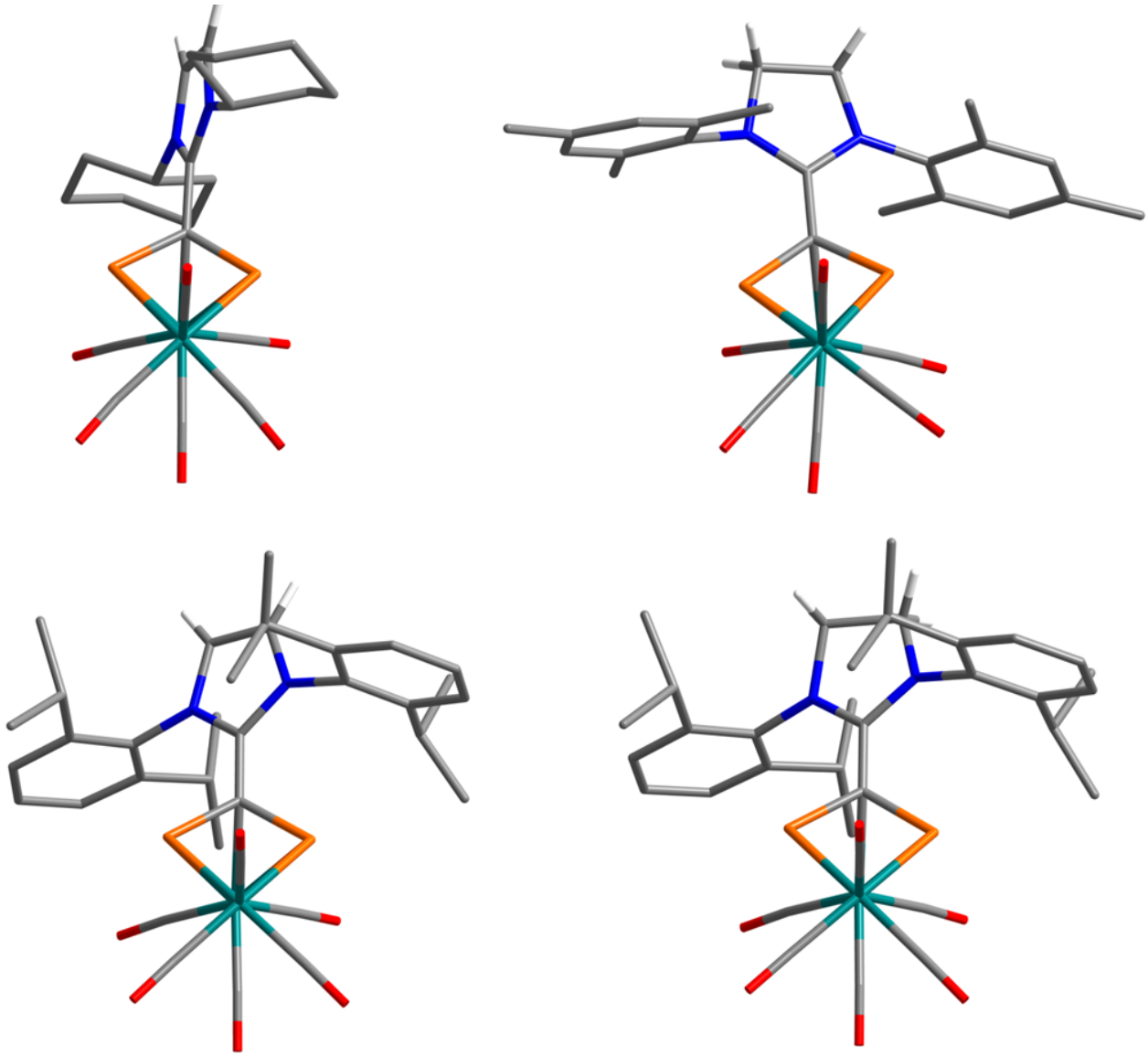

Figure S28. Molecular structures of [$Mn_2(CO)_6(S_2C{\cdot}ICy)$] (**6**) (top left), [$Mn_2(CO)_6(S_2C{\cdot}SIMes)$] (**8**) (top right), [$Mn_2(CO)_6(S_2C{\cdot}IDip)$] (**9**) (bottom left) and [$Mn_2(CO)_6(S_2C{\cdot}SIDip)$] (**10**) (bottom right) showing their staggered conformation

Part 4 – Bibliography

1 L. Delaude, A. Demonceau and J. Wouters, *Eur. J. Inorg. Chem.*, 2009, 1882–1891.

2 Bruker, *APPEX II, Bruker AXS Inc.*, Madison, WI, USA, 2004.

3 R. C. Clark and J. S. Reid, *Acta Crystallogr., Sect. A: Fundam. Crystallogr.*, 1995, **51**, 887–897.

4 M. C. Burla, R. Caliandro, M. Camalli, B. Carrozzini, G. L. Cascarano, L. De Caro, C. Giacovazzo, G. Polidori and R. Spagna, *J. Appl. Cryst.*, 2005, **38**, 381–388.

5 G. M. Sheldrick, *SHELX-97 (SHELXS 97 and SHELXL 97), Programs for Crystal Structure Analyses*, University of Göttingen, Göttingen (Germany), 1998.

6 G. M. Sheldrick, *SADABS, Programs for Scaling and Correction of Area Detection Data*, University of Göttingen, Göttingen (Germany), 1996.

7 H. Putz and K. Brandenburg, *Diamond - Crystal and Molecular Structure Visualization*, Crystal Impact, Bonn (Germany), 2008.

8 T. F. Beltrán, G. Zaragoza and L. Delaude, *Dalton Trans.*, 2016, **45**, 18346–18355.